Michael Ebner, BSc

Photovoltaic cells based on cellulose sheets and cellulose fibers

MASTER THESIS

For obtaining the academic degree
Diplom-Ingenieur

Master Programme of
Technical Physics

Graz University of Technology

Supervisor:

Ao.Univ.-Prof. Mag. Dr.rer.nat. Robert Schennach

Institute of Solid State Physics

Graz, April 2016

EIDESSTATTLICHE ERKLÄRUNG

AFFIDAVIT

Ich erkläre an Eides statt, dass ich die vorliegende Arbeit selbstständig verfasst, andere als die angegebenen Quellen/Hilfsmittel nicht benutzt, und die den benutzten Quellen wörtlich und inhaltlich entnommenen Stellen als solche kenntlich gemacht habe. Das in TUGRAZonline hochgeladene Textdokument ist mit der vorliegenden Masterarbeit/Diplomarbeit/Dissertation identisch.

I declare that I have authored this thesis independently, that I have not used other than the declared sources/resources, and that I have explicitly indicated all material which has been quoted either literally or by content from the sources used. The text document uploaded to TUGRAZonline is identical to the present master's thesis/diploma thesis/doctoral dissertation.

_____ _____

Datum / Date Unterschrift / Signature

Acknowledgement

Firstly, I would like to thank my supervisor Ao.Univ.-Prof. Mag. Dr.rer.nat. Robert Schennach for giving me the chance to write my master thesis about the exciting topic of organic solar cells. I would also like to thank for his advice and assistance through the entire master thesis.

A special thanks-giving to Dipl.-Phys. Dr.rer.nat. Bettina Friedel for her support and ideas, which have helped me a lot. Furthermore, I would also like to thank MSc. Tina Chien who has provided me the electrical resistiviy measurements for the fibers.

At the end I would like to thank my whole family for their endless support through my entire period of study. Finally, the biggest thanks go to my companion through life, Tanja, for supporting all my adventures and misadventures along the way and of course for giving us our son, Eliah.

Abstract

Solar cells are becoming more and more important in terms of generating electrical energy out of renewable energy sources, because solar energy (sun) is available in unlimited disposal. Within this master thesis solar cells based on organic materials were produced due to their advantages of low cost, flexibility and lightness against inorganic solar cells. But because of the disadvantages like low efficiency and short lifetime towards inorganic solar cells, organic solar cells still have problems to reach commercial success.

This master thesis describes the fabrication and characterization of organic solar cells based on cellulose sheets and cellulose fibers. So for the organic solar cells based on cellulose sheets, unrefined soft wood kraft pulp (cellulose) "Monopol X" produced by Mondi Frantschach was used as a substrate. The substrate was coated with silver nanowires via dip-coating to make them conductive and therefore provide a semitransparent conductive substrate. Then as hole conducting layer $PEDOT{:}PSS$ was deposited via drop casting. After that $P3HT$ and $PC_{60}BM$ diluted in chlorobenzene was used as the active layer for the energy conversion of the device. And in the end aluminum (Al) was evaporated as the upper electrode by thermal evaporation. For the organic solar cells based on cellulose fibers, hollow regenerated cellulose fibers with a diameter of 2.1 dtex (about 20 μm) and a length of about 4 cm were used as a substrate. The other fabrication steps were the same as for the organic solar

cells based on cellulose sheets.

To characterize the fabricated organic devices different investigation methods have been applied. First the resistance of the conductive cellulose sheets and cellulose fibers was measured, then the transmission spectra for the conductive cellulose sheets were recorded and in the end the current-voltage characteristics of the organic devices with and without illumination were measured. What has been found is, that the conductive cellulose sheets can be used as semitransparent electrode for organic photovoltaic cells and the fabricated devices showed quite proper performance. Against that the organic solar cells based on cellulose fibers showed fairly poor values. The problem was that the aluminum electrode is not transparent and therefore a disadvantageous overall geometry had to be used.

Kurzfassung

Solarzellen gewinnen immer mehr an Bedeutung bezüglich der Erzeugung elektrischer Energie aus erneuerbaren Energiequellen, da die Solarenergie (Sonne) unlimitiert zur Verfügung steht. Innerhalb dieser Masterarbeit wurden Solarzellen basierend auf organischen Materialien hergestellt, da sie die Vorteile von geringen Kosten, Flexibilität und geringes Gewicht gegenüber anorganischen Solarzellen haben. Aber durch Nachteile wie geringe Effizienz und kurze Lebenszeit gegenüber anorganischen Solarzellen, haben organische Solarzellen noch immer Probleme kommerziellen Erfolg zu erzielen.
Diese Masterarbeit beschreibt die Herstellung und Charakterisierung von organischen Solarzellen basierend auf Zelluloseblättern und Zellulosefasern. Also für die organischen Solarzellen basierend auf Zelluloseblättern wurde als Substrat nicht raffinierter Weichholzzellstoff (Zellulose), hergestellt durch Mondi Frantschach verwendet. Um das Substrat leitfähig zu machen, wurde es mit Silber-Nanodrähten beschichtet, die mittels Tauchbeschichten aufgetragen wurden, dadurch konnte ein semitransparentes leitendes Substrat bereitgestellt werden. Danach wurde durch Auftropfen $PEDOT{:}PSS$ als Löchertransportschicht aufgetragen. Daraufhin wurden $P3HT$ und $PC_{60}BM$ verdünnt in Chlorbenzol als aktive Schicht verwendet, die für die Energieumwandlung zuständig ist. Zum Schluss wurde Aluminium (Al) als obere Elektrode durch thermische Verdampfung aufgebracht. Für die organischen Solarzellen

basierend auf Zellulosefasern wurden als Substrat hohle regenerierte Zellulosefasern mit einem Durchmesser von 2.1 dtex (zirka 20 μm) und einer Länge von 4 cm verwendet. Die anderen Herstellungsschritte waren dieselben wie für die organischen Solarzellen basierend auf Zelluloseblättern.
Um die hergestellten organischen Bauteile zu charakterisieren wurden verschiedene Untersuchungsmethoden angewendet. Als Erstes wurde der elektrische Widerstand der leitfähigen Zelluloseblätter und Zellulosefasern bestimmt, dann wurden Transmissionsspektren von den leitfähigen Zelluloseblättern aufgenommen und zum Schluss wurden die Stom-Spannungs-Charakteristiken der organischen Geräte einmal mit und einmal ohne Beleuchtung gemessen. Was gezeigt wurde, ist , dass die leitfähigen Zelluloseblätter als semitransparente Elektrode für organische Solarzellen verwendet werden können und dass die hergestellten Geräte durchaus ansprechende Leistung zeigten. Dagegen zeigten die organischen Solarzellen basierend auf Zellulosefasern ziemlich schlechte Werte. Das Problem hierbei war, dass die Aluminiumelektrode nicht transparent ist und somit eine nachteilige Gesamtgeometrie verwendet werden musste.

Contents

1 Introduction

In times of smartphones, tablets and other intelligent electronic devices the demand for energy is increasing rapidly and globally [1]. The future global energy demand is depicted in figure 1.1 and as one can see the world will require 45 percent more energy in 2035 than in 2011 [1].

To deal with this increase, you could probably burn more oil, but this would of

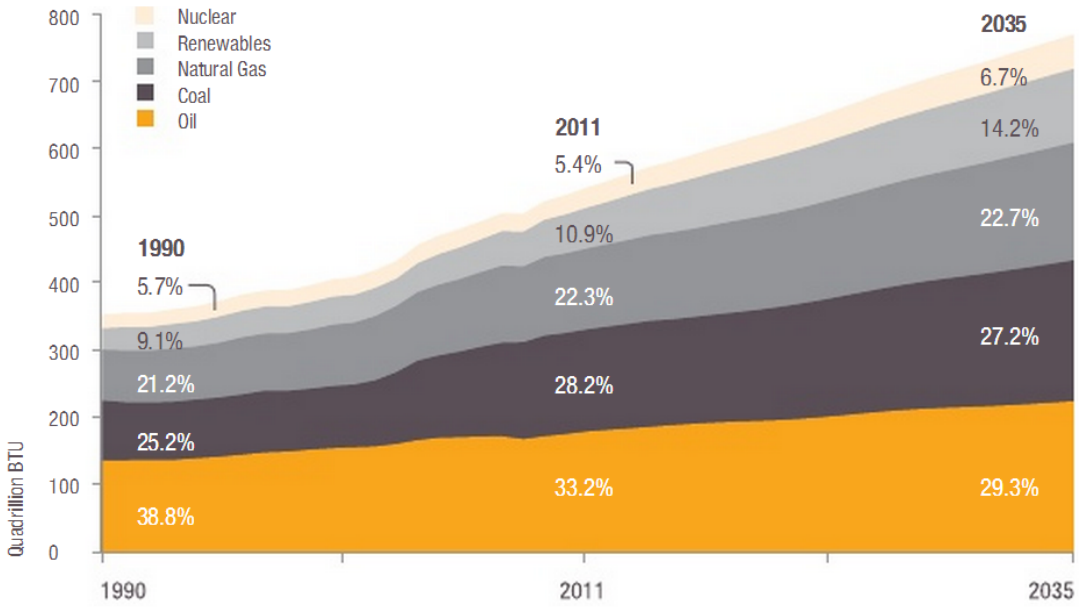

Figure 1.1: Future Global Energy Demand - the world will require 45 percent more energy in 2035 than in 2011 [1]

course support the global warming [2]. Therefore, one of the ways to solve this problem is using renewable energy instead of energy generated by fossil fuel technology. Renewable energy has a lot of benefits against fossil fuels [3, 4]. The most important advantage is that renewable energy technologies are neat energy sources and by using them instead of burning fossil fuels the global warming emission will be reduced significantly [3, 5].

The fact that impurities caused by burning fossil fuels are brought in connection with respiratory problems, heart attacks and cancer leads to another advantage, because it has been provided that renewable energy technologies will reduce these health problems and therefore improve the public health [3, 5]. So using renewable energy will improve human well-being and the global welfare [4].

Another benefit against carbon-intensive energy sources is that renewable energy will never run out, so even the children of your children will be able to use it [3, 5]. As a consequence of this inexhaustible energy supply, renewable energy prices will also be relatively stable over time [3].

Whilst fossil fuel technologies are normally mechanistic and therefore capital intensive, renewable energy technologies are more research intensive, which means that more jobs are created since the research work generally requires more jobs [3]. As a positive side effect the global gross domestic product (GDP) would also grow [4].

The next advantage deals with the topic of energy security. Today a lot of countries depend on foreign oil suppliers and therefore this high dependency on oil-producing countries is not good for nations energy security. With renewable energies this problem could be solved, because in principle each country could even produce energy for themselves [5].

The used renewable energy technology within this master thesis is photovoltaic, which is one of the tidiest, most usable and encouraging renewable energies

by using unlimited light from the sun to generate electricity. Such photovoltaic cells are used in many different application fields like in the building sector, the agricultural sector and for example in the textile industry. When talking about textile industry, one thinks more and more mainly on organic photovoltaic cells especially on organic photovoltaic fibers, because of their preferable features such as low cost, lightness and flexibility (see figure 1.2) [6]. To use the

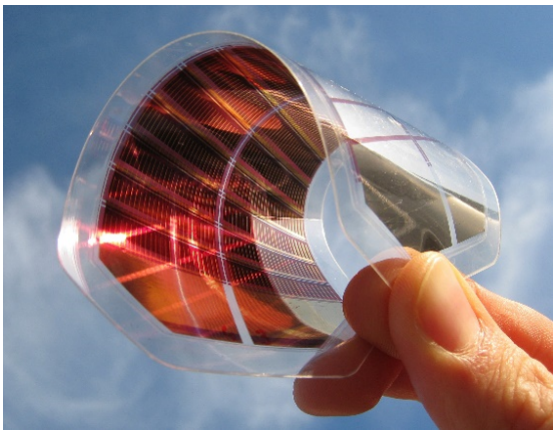

Figure 1.2: Folded organic photovoltaic cell to show flexibility [7]

photovoltaic technology in the textile industry the photovoltaic materials can be directly integrated onto textile structures and by that the photovoltaic textile becomes ready for power harvesting. Therefore, this master thesis presents an organic photovoltaic fiber based on a regenerated cellulose fiber, which are readily found in common textiles. In the following the architecture, the production, and the electronic properties of these viscose fiber based solar cells will be discussed. The methods used in this paper focus on scalability in terms of being usable in a roll-to-roll process as it has been outlined in [8].

2 Theoretical background

This chapter should give an overview about organic semiconductors and especially their application in organic solar cells. Additionally also the depositing techniques used in this master thesis will be described and in the end also the electrical characterization method to determine the performance of the produced organic solar cells.

2.1 Organic semiconductors

Organic semiconductors count to the organic solid states, which can be molecular crystals as well as thin layers of polymers and small organic molecules. The most important force for the cohesion of the organic solid states is the Van-der-Waals-force.

Opposed to inorganic semiconductors, where the excitations from valence band to the conductive band are responsible for semi-conducting properties, for the organic semiconductors the transitions between the highest occupied molecular orbital ($HOMO$) and the lowest unoccupied molecular orbital ($LUMO$) are accountable for the semi-conducting properties (see figure 2.1) [6]. The band gap is the energy difference between $HOMO$ and $LUMO$:

$$E_{gap} = E_{LUMO} - E_{HOMO} \tag{2.1}$$

In general, the carriers are in organic, non-single crystalline semiconductor,

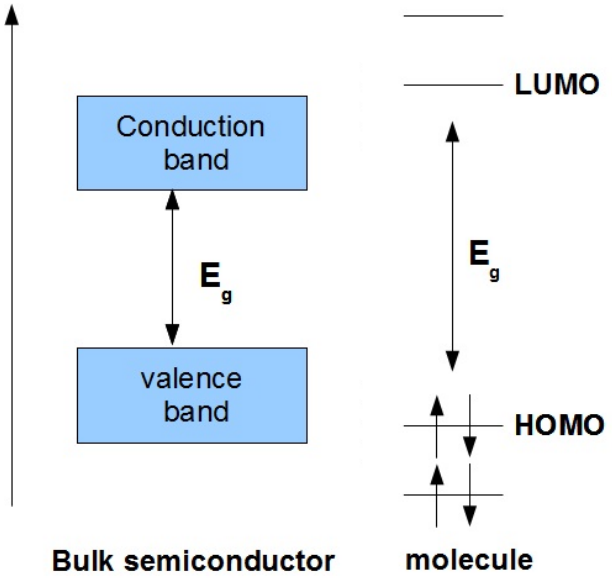

Figure 2.1: Electronic structure of single molecules and bulk semiconductors [9]

such as they are available after the production of thin films, localized on the molecules. The transport operations can only take place by hopping of charge carriers between the localized states of adjacent molecules. To jump over the potential barriers between the molecules, the charge carriers need extra energy which is supplied via thermal excitation, this transport process is called "thermally assisted hopping" [10].

A special property of organic semiconductors is that they have high exciton binding energies. While the exciton binding energies have in inorganic semiconductors values in the range of 10 meV and therefore do not play an important role, excitons in organic semiconductors with binding energies from 0.4 eV to 1.2 eV are largely decisive for the electrical properties [10].

Excitons are quasiparticles, they can move through a solid and therefore transport energy. They represent electron-hole pairs which are bound via the coulomb interaction, due to the opposed charges. While the electron is located

in the *LUMO*, the hole is located in the *HOMO* and a charge transport can only take place when the two charge carriers are separated and propagate to the opposing electrodes.

2.2 Organic solar cells

Solar cells are large area photo diodes, which are specifically optimized to the spectrum of the sun to directly gain electrical energy from sunlight [11].

2.2.1 Structure

In figure 2.2 one can see the basic structure of an organic solar cell. As one can see a typical organic solar cell consists of one or several photoactive materials sandwiched between two electrodes. Bilayer cells like in the figure contain two active layers in between the conductive electrodes, these two layers have different electron affinity and ionization energies. The layer with higher electron affinity and ionization potential is the electron acceptor, the other layer is the electron donor. This structure is also called a planar donor-acceptor heterojunction. Like it is usual in the thin film technology, the active layers are applied on a transparent contact layer and finished with a reflective electrode [12].

2.2.2 Working principle

This short chapter will present the basic working principle of an organic solar cell, which is shown in figure 2.3.
The light is usually mainly absorbed in the so-called donor material, which is a

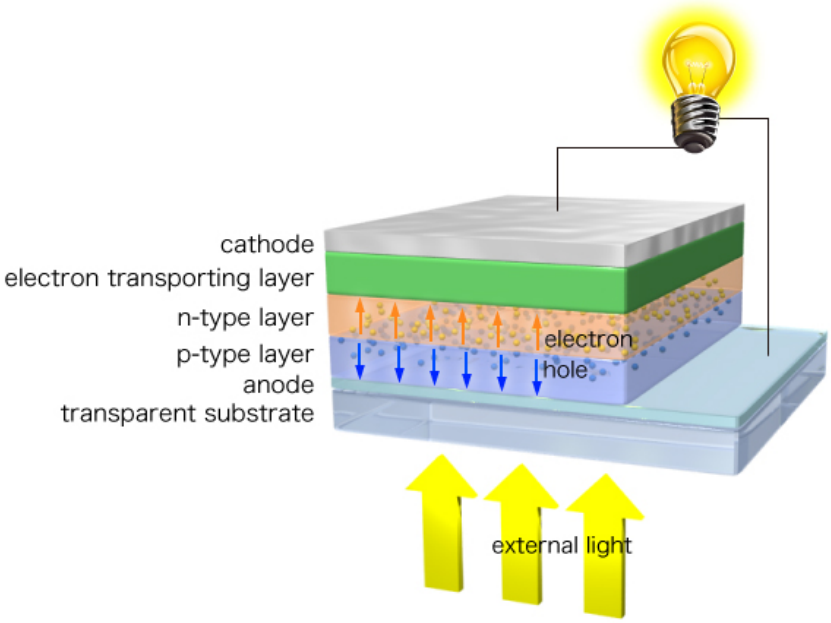

Figure 2.2: Basic structure of an organic photovoltaic cell [13]

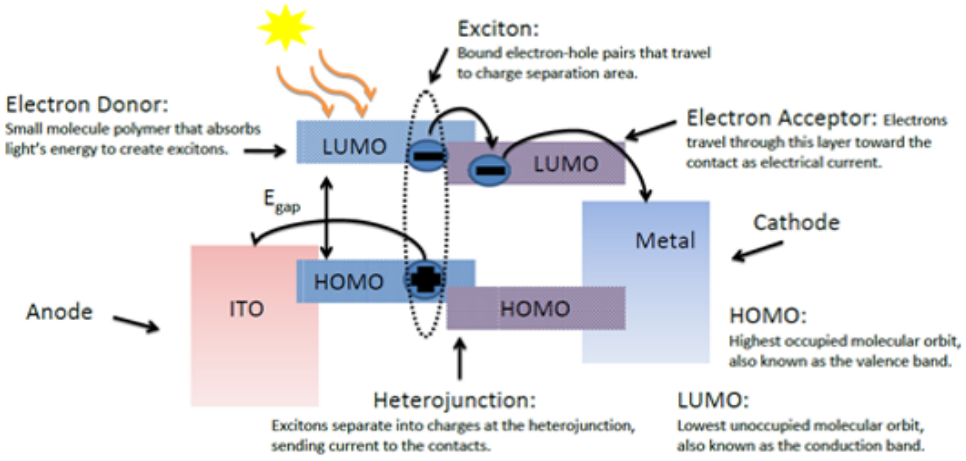

Figure 2.3: Working principle of an organic photovoltaic cell [14]

hole conducting little molecule. When the donor absorbs a photon, an excited state, an electron-hole pair, is created. As mentioned before these electron-hole pairs can be considered as an exciton. These photo generated excitons now can move via diffusion within the donor towards the connector to the second material, the acceptor, which is in common strongly electronegative. The energy difference between the electron niveau of the donor and the acceptor niveau has to be bigger than the exciton binding energy, so as to launch a charge transfer from donor to acceptor material. If an exciton diffuses in the direction of the donor-acceptor heterojunction, it is energetically advantageous that the electron is transferred to the acceptor material. Opposed to the electron, the hole remains on the donor, which means that the exciton is dissociated and therefore electron and hole are now spatially divided [15].
Although electron and hole stay now on separate sites, they are still coulombically bound. For breaking this coulomb bond an additional step is needed. An electric field is necessary to vanquish the coulomb interaction. This extra electric field is strongly dependent on the discharge energy difference between the two electrode materials. After that the last step is the transport of the charge carriers to the respective electrodes, which means the electron moves across the acceptor to the cathode and the hole across the donor to the anode [15].

2.2.3 Critical design issues

Based on the working principle of an organic solar cell, there are 4 critical design issues regarding the construction of an organic solar cell:

1. The first critical design issue is about the exciton generation, which is quantified by the exciton generation efficiency η_{Abs}. It indicates the

efficiency about how much of the incoming photons have produced excitons [16, 17].

2. The second critical design issue is about the exciton diffusion to interface, here the coefficient η_{ExDiff} gives the part of the excitons which are capable to hit the donor/acceptor junction and divide into still coulombically bound electron-hole pairs. The coefficient is dependent on the distance the exciton has to overcome before reaching the donor/acceptor junction, because excitons have small diffusion length of about 10 nm [18]. If they can reach a donor-acceptor interface before recombination a charge transfer state is formed at the interface. This means, that the electron is transfered from the the donor to the acceptor. The hole remains in the donor [16, 17].
3. This electron-hole pair is still coulombically bound to the interface. The bonded electron-hole pairs need to be separated into free charge carriers. This is referred to the separation efficiency η_{Sep}. It strongly depends as said before on the workfunction difference between the electrode materials and needs to be higher than the coulomb attraction [16, 17].
4. The last critical design issue is the charge transport to the electrodes. The electron moves through the acceptor to the cathode and the hole through the donor to the anode. η_{Coll} determines the efficiency of bulk transport of the free charges to their respective electrodes and their collection at the same. It is limited by interface and contact resistance [16, 17].

To get now the overall efficiency one can easily multiply all efficiencies:

$$\eta = \eta_{Abs} \cdot \eta_{ExDiff} \cdot \eta_{Sep} \cdot \eta_{Coll} \tag{2.2}$$

2.2.4 Bulk morphology

For the second critical design issue η_{ExDiff} the donor-acceptor structure in the active layer becomes most important. For example an easy bilayer heterojunction organic solar cell, as depicted in figure 2.4(a), is not a good chosen bulk morphology because only a region in the order of 10 nm (due to the small diffusion length of the exciton) on both sides of the interface would generate a current, while around 100 nm of the layer is necessary to absorb most of the photons [19].
So it is necessary to make the junction area big enough, this can be accomplished when using phase separation in the active region. For instance it is possible to create such an optimal active layer by using lithography as a depositing method, then the layer may look like a comb which can be seen in figure 2.4(b) [19].
It is kind of funny that of all things the simplest method for manufacturing the optimal active layer is also the best method. One can easily dissolve and mix the two active materials (donor, acceptor) in an usual solvent and then simply drop-cast the active layer from this compound. After a drying period the active layer materials divide into two individual phases as imaged in figure 2.4(c), this bulk morphology is named bulk heterojunction (BHJ) [19].
Also for this master thesis bulk heterojunction was used as a bulk morphology.

2.3 Depositing layer methods

In order to produce the organic photovoltaic cells, for the respective layers, different coating methods were used. To establish conductive cellulose substrates

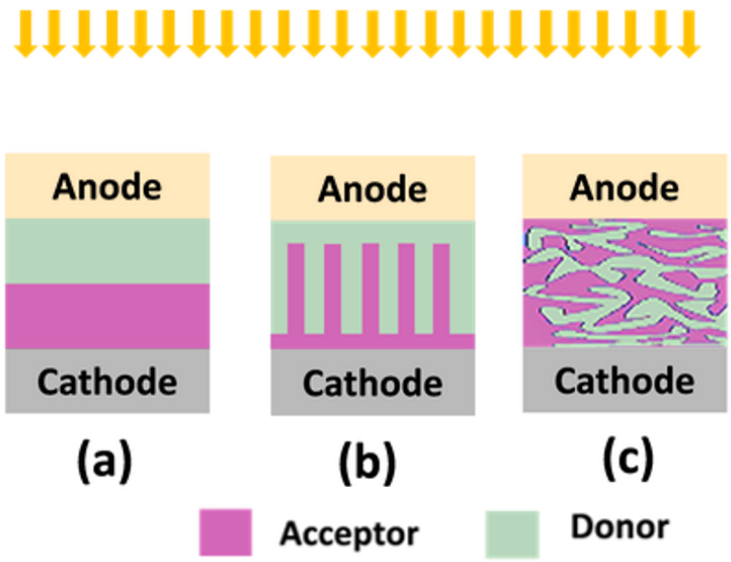

Figure 2.4: Different possible bulk morphologies from an organic photovoltaic cell [19]

dip-coating was used for depositing silver nanowires on the cellulose substrates. For the active layers ($PEDOT$:PSS and $P3HT$:$PC_{60}BM$) drop-casting was selected as a depositing method. The last layer, the aluminum electrode, was deposited using the thermal evaporation process, which is the only process where a vacuum chamber is necessary.

2.3.1 Dip-coating

As mentioned before for depositing the silver nanowires dip-coating was used as a coating technique, for this the principal process is depicted in figure 2.5. First the substrate is dipped in the coating material solution at a certain speed (v_{dip}). After that the substrate stays in the solution for a specific time (t_{stop}) and the coating material begins to build up on the substrate. The next step is the most important step in the dip-coating process, the substrate is withdrawn with a predefined withdrawal speed (v_{wd}). During this step

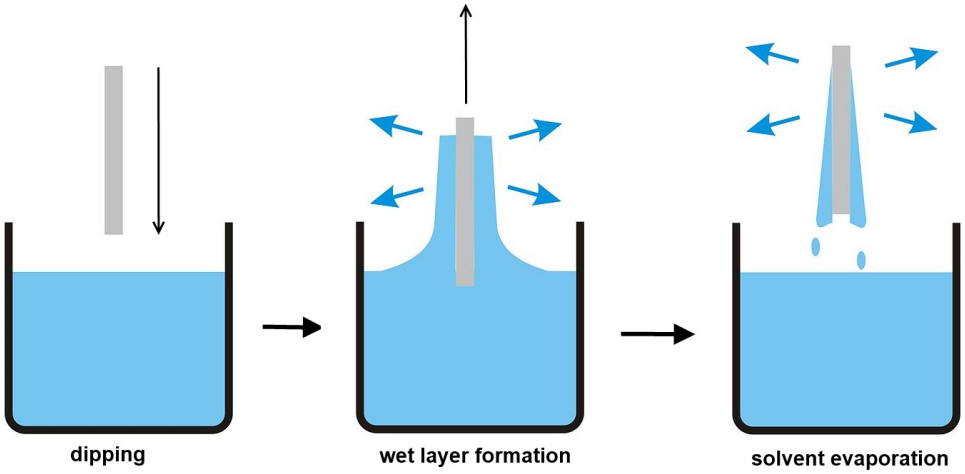

Figure 2.5: Dip-coating method for depositing thin films

the coating material deposits itself on the substrate while it is withdrawn. The withdrawal speed is the key parameter for defining the final thin layer thickness [20]. The final thickness can also be calculated theoretically using the Landau-Levich equation:

$$h = 0.94 \frac{(\eta \cdot v_{wd})^{2/3}}{(\rho \cdot g)^{1/2} \cdot \gamma_{LV}^{1/6}} \tag{2.3}$$

with the thickness h, the withdrawing speed v_{wd}, the surface tension of the liquid γ_{LV}, the density ρ, the viscosity η and the gravitation constant g.

2.3.2 Drop-casting

The drop-casting method is a very simple method, the basic process is shown in figure 2.6. As one can see it is only dropping of dispersion with a micro-pipette and afterwards spontaneous solvent evaporation. The final film thickness depends on the volume of the solution and the solution concentration. In addition to the simplicity of this depositing method another advantage is

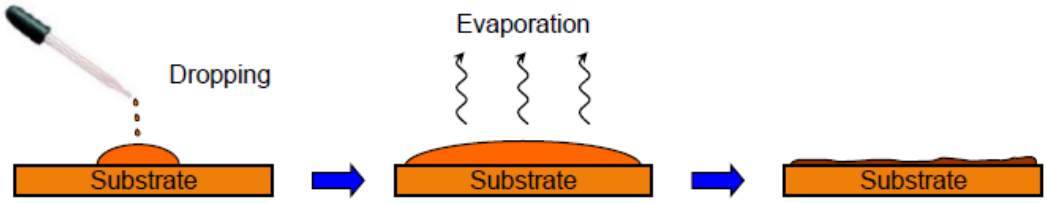

Figure 2.6: Drop-casting method for depositing thin films [21]

that no material is wasted. Disadvantages of this thin film technique are that the thickness is hard to control, the thin film has a poor uniformity and this method has limitations in large area coverage. To compensate the poor uniformity one can heat up the substrate after drop-casting to speed up the evaporation process and improve through that the film morphology.

2.3.3 Thermal evaporation

For creating the aluminum top electrode thermal evaporation under vacuum was used as a depositing method, the experimental setup for the thermal evaporation process is depicted in figure 2.7. During the thermal evaporation process the source material is heated up to temperatures near the boiling point. At this point single atoms, atom clusters or molecules start to evaporate and move through the vacuum chamber. Due to the experimental arrangement between the evaporation source and the substrate, the material steam starts to condensate on the cooler opposing substrate. Afterwards on the substrate a thin layer of the vaporized material starts to grow. A disadvantage of the thermal evaporation process is that the material vapor in the vacuum chamber propagates in all directions and therefore some of the source material also deposits on the vessel wall of the recipient.
As already mentioned the thermal evaporation is a high vacuum process, for

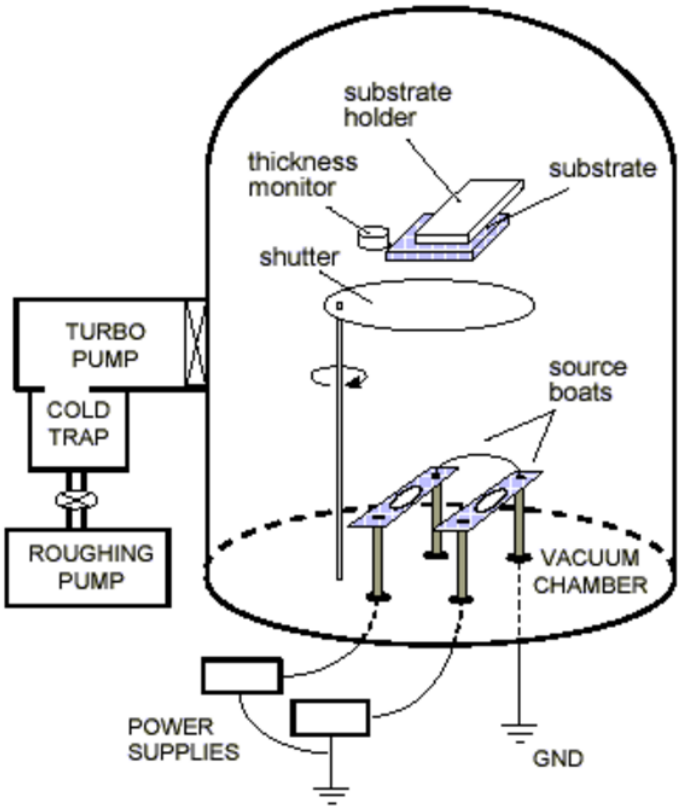

Figure 2.7: Thermal evaporation: experimental setup for depositing thin films [22]

receiving such a high vacuum a turbo-molecular pump as depicted in figure 2.7 is used. Typical process pressures are in the range of (10^{-5} - 10^{-6}) mbar, these pressures are necessary because the pressure of the process needs to be lower than the gas pressure of the depositing material and also within this pressure range the mean free path is much bigger than the distance between substrate and evaporation source.
The shutter which can be seen in figure 2.7 is needed for covering the substrate against the evaporation of unwanted organic materials and finally also a quartz sensor, used as a thickness monitor (see figure 2.7), is required to control the whole evaporation process.
In the process of depositing aluminum as a cathode one also had to take account of two key factors:

1. On the one hand the aluminum source must not be too hot, because otherwise the polymers can be damaged due to the heat.
2. On the other hand the aluminum atoms are not allowed to have a too high kinetic energy, if not they could damage the surface of the polymers or they could penetrate the surface. This could lead to formation of short circuit paths through the polymers and therefore to an increase of leakage current.

   To prevent this it is necessary to work with a minimum aluminum source temperature, which leads to a low depositing rate. However in the vapour deposition of the 100 nm thick aluminum layer a damage of the substrates is not very likely, therefore the depositing rate was set to (5-10) nm/s.

2.4 Electrical characterization

To determine the performance of an organic photovoltaic cell current-voltage (I-V) measurements under dark conditions and under illumination are accomplished. In figure 2.8 such a typical current-voltage curve is shown.
When there is no current between the two contacts of an organic photovoltaic

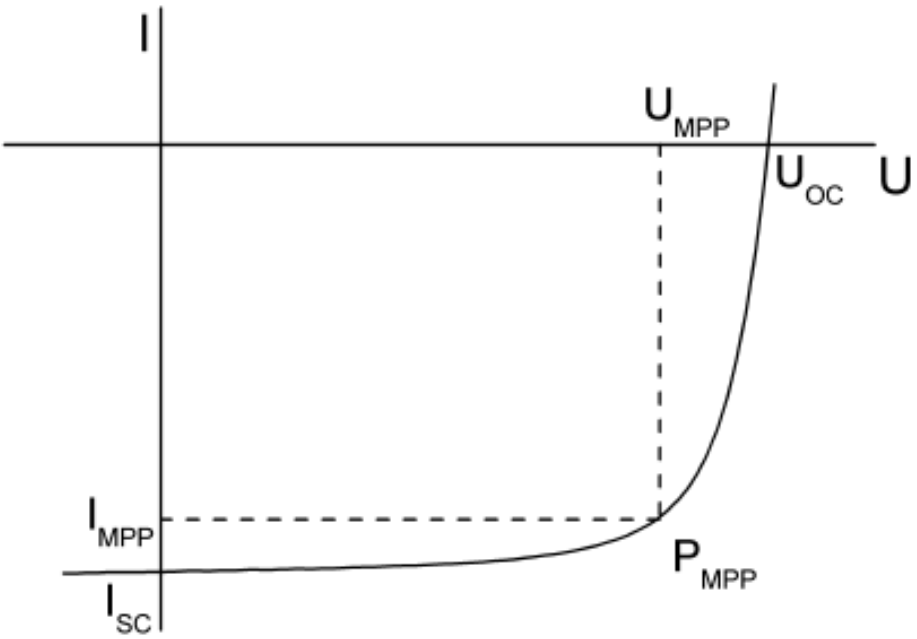

Figure 2.8: Current-Voltage (I-V) characteristics of a illuminated organic photovoltaic cell with the parameters short-circuit current I_{SC}, open-circuit voltage U_{OC}, maximum power point P_{MPP} with the values for current I_{MPP} and voltage U_{MPP} [23]

cell, the open-circuit voltage U_{OC} is measurable. Against that if you short-circuit the two electrodes, one can measure a current, the short-circuit current I_{SC}. The operational area of an organic photovoltaic cell is the scope of bias from 0 to U_{OC} where the cell is providing power [24]. To get the power of an

organic solar cell, one can use the simple formula:

$$P = U \cdot I \tag{2.4}$$

Now the point where P reaches the maximum is called the maximum power point P_{MPP}, which is determined by the specified values for current I_{MPP} and voltage U_{MPP}.The maximum power point P_{MPP} is also shown in figure 2.8. With the current I_{MPP} and voltage U_{MPP} at maximum power plus the short-circuit current I_{SC} and the open-circuit voltage U_{OC} the fill factor FF can be calculated:

$$FF = \frac{U_{MPP} \cdot I_{MPP}}{U_{OC} \cdot I_{SC}} \tag{2.5}$$

The fill factor is an important parameter for the goodness of organic solar cells, it gives information about the power conversion efficiency of an organic solar cell. The next quantity is the power conversion efficiency η, which determines how much of the radiated energy was converted to usable electrical energy. The power conversion efficiency η can be calculated using the equation:

$$\eta = \frac{U_{MPP} \cdot I_{MPP}}{P_L} = \frac{FF \cdot U_{OC} \cdot I_{SC}}{P_L} \tag{2.6}$$

where P_L is the radiated luminous power. Now with η and the three parameters U_{OC}, I_{SC}, FF one can provide important information about the performance of an organic solar cell.

2.5 Materials

In the chapters 3.1 and 4.1 the fabrication of the organic photovoltaics based on cellulose sheets respectively fibers is described. The materials used for the fabrication will be presented in this chapter. Initially the substrates will be described shortly and also the manufacturing process of a regenerated viscose

cellulose fiber as used in this master thesis will be explained. Afterwards the polymers used for the active layer are presented and subsequently the *PEDOT*:*PSS* hole conducting layer is described.

2.5.1 Substrates

For the organic photovoltaic devices based on cellulose sheets in this master thesis unrefined soft wood kraft pulp called "*Monopol X*" provided by Mondi Frantschach GmbH was used.
For the organic photovoltaic devices based con cellulose fibers, hollow regenerated cellulose fibers with a diameter of 2.1 dtex (about 20 μm) and a length of about 4 cm, named bramante fibers, were used as viscose fibers. The fibers were supplied by Kelheim Fibres GmbH, Kelheim, Germany. In figure 2.9 it is easy to see that the fibers are hollow, the fibers are also segmented to prevent collapse of themselves.

Figure 2.9: Electron microscopy image of the regenerated cellulose fibers used in this study. The fiber diameter is approximately 20 μm. Picture courtesy of Kelheim Fibres GmbH.

Manufacturing process of a regenerated viscose fiber

Within this section it is briefly described how to fabricate a regenerated viscose fiber out of cellulose.
The term "regenerated cellulose fibers" refers to those fibers that are produced through a chemical process from naturally renewable raw materials. The basis for the production of these fibers is provided by cellulose extracted from wood, also known as wood pulp.
The obtained wood pulp now is the source for the next steps, first the wood pulp is dipped in a sodium hydroxide solution (18-22%), as a result alkali cellulose $[C_6H_9O_4 - ONa]_n$ is formed, although a part of the hydroxyl groups release a proton H^+ [25].
Subsequently the alkali cellulose is pressed to dry it a little and then pulped to a crumbly mass, which will rest for 1-2 days (aging). Over the time, the alkali cellulose is digested into smaller pieces (depolymerization). In the next step the alkali cellulose is treated with carbon disulfide, whereby cellulose xanthogenate $[C_6H_9O_4 - OCS_2Na]_n$ is formed, an orange yellow mass also known as "viscose" [25]:

$$[C_6H_9O_4 - ONa]_n + nCS_2 \longrightarrow [C_6H_9O_4 - OCS_2Na]_n \tag{2.7}$$

To obtain now the viscose fibers a spinning solution is needed, therefore the cellulose xanthogenate is dissolved in sodium hydroxide solution (7%) . After that the spinning solution has to ripe 2-3 days, whereas polymerizations take place [25].
After ripening the spinning solution is pressed through fine nozzles in a precipitation bath, containing sulfuric acid $[H_2SO_4]$ and sulfates like sodium sulfate $[Na_2SO_4]$ and zinc sulfate $[ZnSO_4]$. In the precipitation bath, the carbon disulfide molecules, which are bound to the cellulose, split off again for the most part of it. It forms sulfur, hydrogen sulfide, carbon disulfide, sodium

sulfate and finally the desired viscose fibers, which consists of almost pure cellulose. As the last process the fiber has to be washed to free it from the unhealthy substances, and finally it is dried and bleached [25].
Such a fabrication process as described above is shown in detail in figure 2.10.

2.5.2 Electron acceptor

As the electron acceptor for the bulk heterojunction the fullerene derivative $[6,6]$-*phenyl*-C_{61}-*butyric-acid-methyl-ester* called $PCBM$ was chosen. The chemical structure is shown in figure 2.11. Opposing to normal C60-fullerenes it is soluble and therefore can be dissolved with $P3HT$ in the same solvent. While the level of the $HOMO$ is (6.1 - 6.8) eV below the vacuum level, the level of the $LUMO$ is (3.7 - 4.1) eV below the vacuum level, which results in a band gap of approximately 2.7 eV [27].

2.5.3 Electron donor

In this master thesis $Poly(3\text{-}hexylthiophene\text{-}2,5\text{-}diyl)$ called $P3HT$ was used as a electron donor for the bulk heterojunction. The chemical structure is depicted in figure 2.12. While the level of the $HOMO$ is (4.9 - 5.2) eV below the vacuum level, the level of the $LUMO$ is (2.9 - 3.3) eV below the vacuum level, which results in a band gap of approximately 1.9 eV [27].

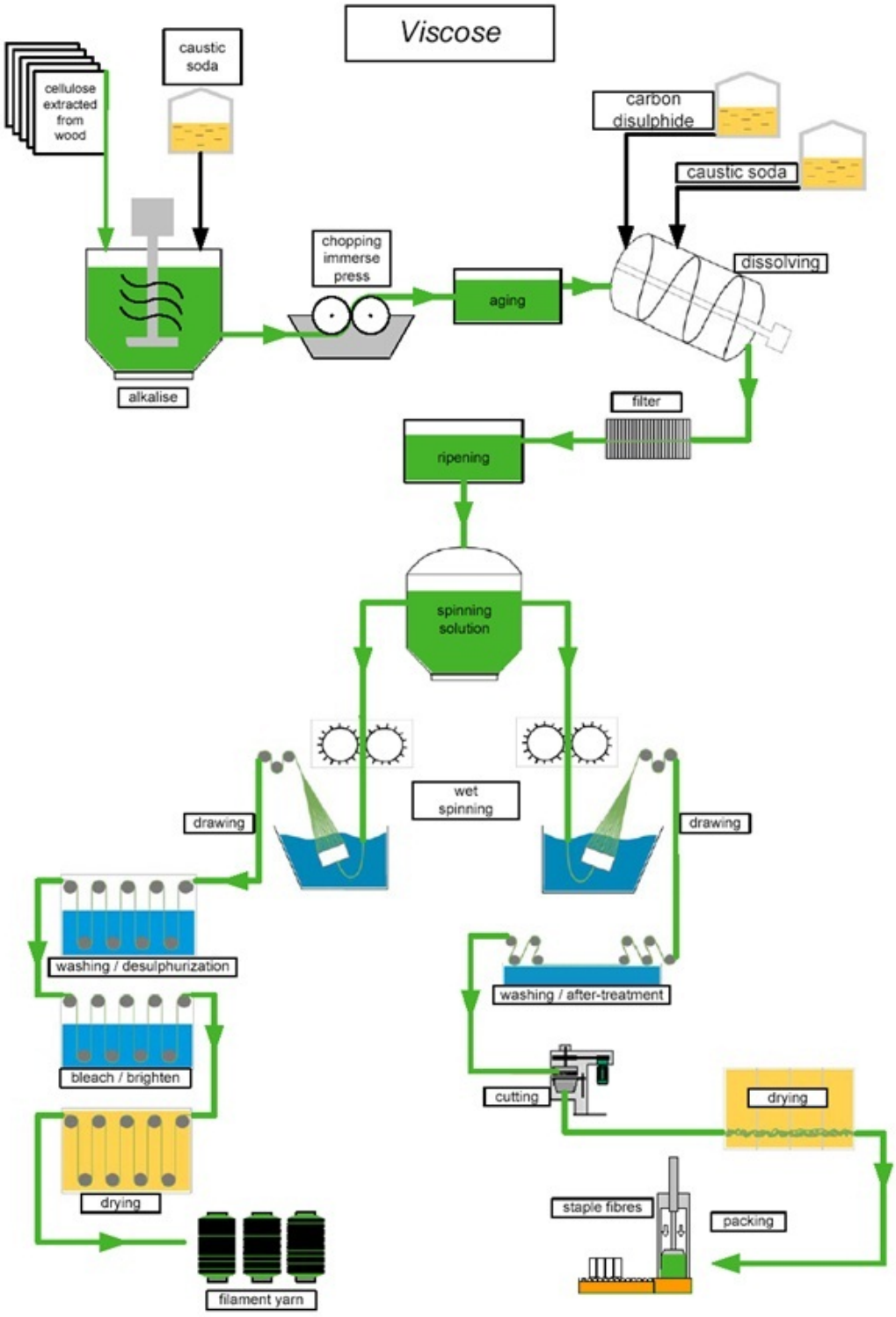

Figure 2.10: Process for fabricating regenerated viscose fibers [26]

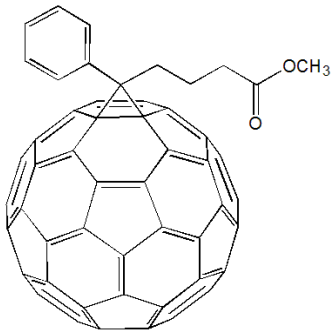

Figure 2.11: Chemical structure of *PCBM* [28]

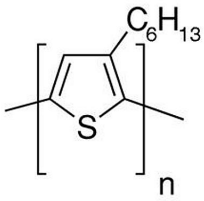

Figure 2.12: Chemical structure of *P3HT* [29]

2.5.4 Hole conducting layer

As a hole conducting layer between the electrode and the bulk heterojunction a water soluble conjugated polymer consisting of a mixture of Poly(3,4-ethylenedioxythiophene) (*PEDOT*) and sodium polystyrene sulfonate (*PSS*). The polymer is then named *PEDOT*:*PSS*, *PSS* is necessary to make it soluble in water. The chemical structure is depicted in figure 2.13. With a work function of 5.2 eV and a band gap of approximately 1.5 eV it serves beside hole conducting layer also as an electron blocking layer [27].

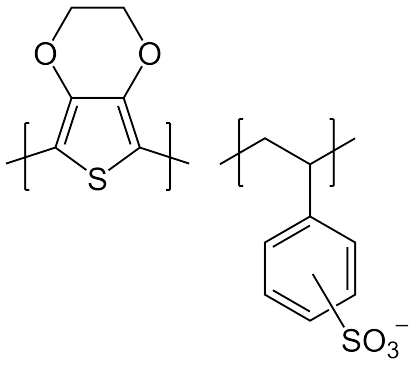

Figure 2.13: Chemical structure of *PEDOT* : *PSS* [30]

3 Organic photovoltaic cells based on cellulose sheets

3.1 Fabrication process

In this chapter the fabrication process for an organic photovoltaic cell based on cellulose sheets will be presented. To have a better overview, the whole fabrication process was depicted in a flowchart (Figure 3.1).

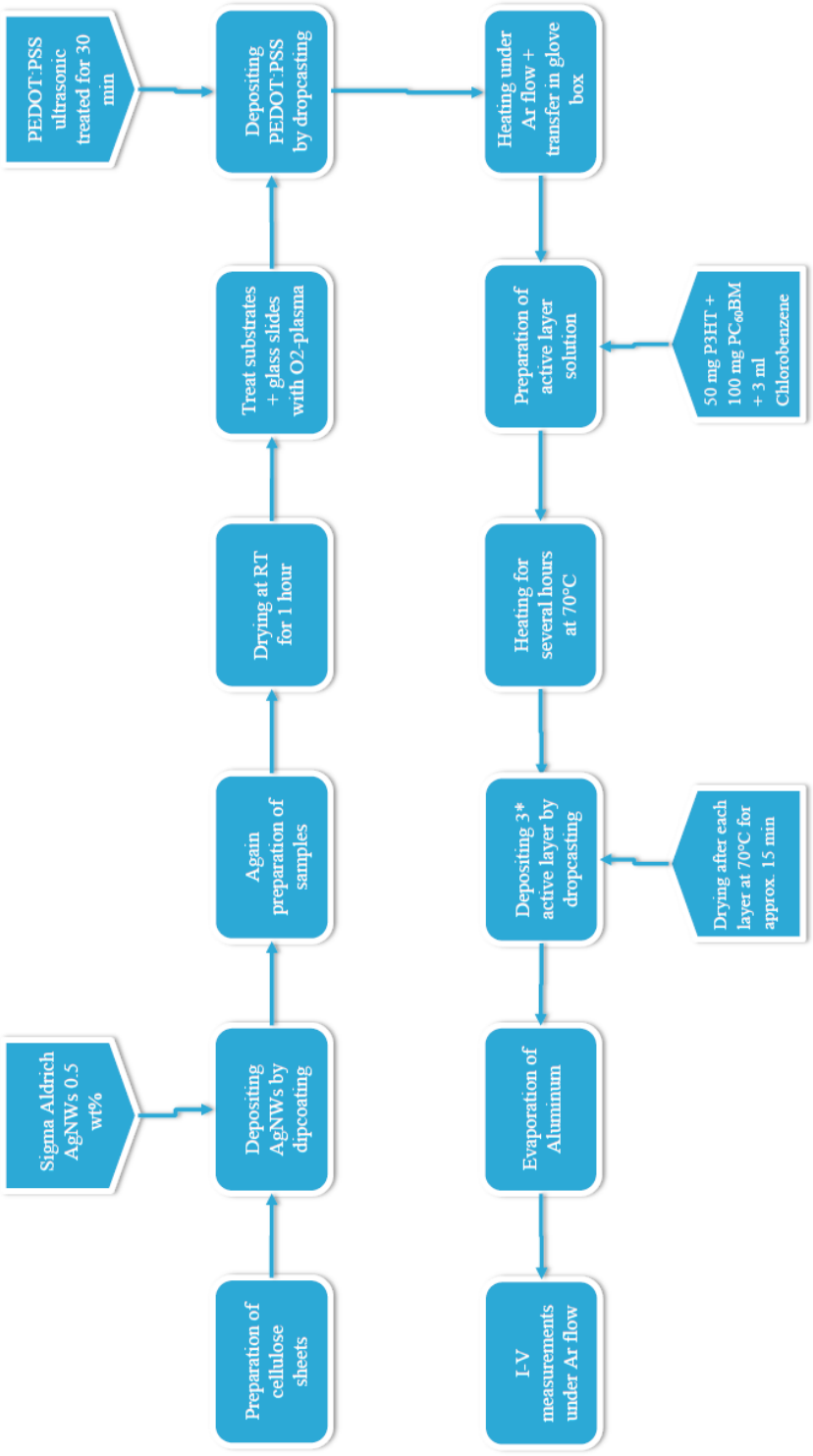

Figure 3.1: Flowchart for the fabrication process of the cellulose sheets

3.1.1 Preparation of the cellulose substrates

As a substrate unrefined soft wood kraft pulp (cellulose) "Monopol X" produced by Mondi Frantschach was used. The cellulose substrates were cleaned with compressed air and then cut to a size of (25 x 40) mm^2.

3.1.2 Depositing silver nanowires by dip coating

Past preparation of the cellulose substrates, electrically conductive cellulose sheets were established using silver nanowires as a conductive layer. Therefore a suspension of silver nanowires (diameter: 115 nm, length: 20 - 50 μm) in isopropanol supplied by Sigma-Aldrich was used. The inner electrode on the cellulose sheets surface was made by dip coating the sheets in this supplied suspension. As a dip coater the SDI Nano DIP ND-0407 dip-coater was used (see figure3.2). Before the dip coating process the substrates were folded in half to receive silver nanowires only on one side of the cellulose sheets. After the dip coating process and before drying the cellulose sheets have been unfolded and then dried at room temperature for 1 hour [16].
The detailed parameters for the dip coating process can be found in table 3.1.

Table 3.1: Detailed parameters for the dip coating process of the cellulose sheets

parameter	**value**
v_{dip} $(\mu m/s)$	500
t_{stop} (s)	30
v_{wd} $(\mu m/s)$	33.33

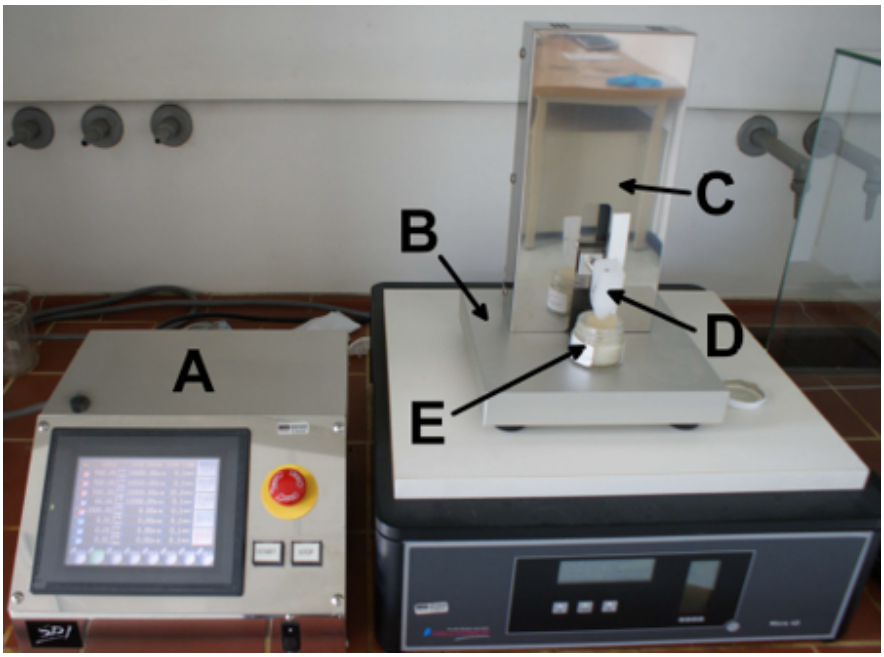

Figure 3.2: SDI Nano DipCoater with control unit (A), stage (B), moveable arm (C), probe holder (D) and the dip coating solution (E) [16]

3.1.3 Preparation of the conductive cellulose substrates

After depositing silver nanowires, the cellulose substrates were prepared again. Therefore the cellulose substrates with the silver nanowires were cut ot a size of (18 x 18) mm^2. Additionally microscopy slides were cleaned and also cut to a size of (18 x 18) mm^2. The microscopy slides were only for better handling necessary. After cutting the coated cellulose substrates, on the side towards the silver nanowires conductive silver contact points were set to link the anode after fabrication for making I-V characterization of the organic photovoltaic cells. The conductive silver contact points need to dry at room temperature for about 1 hour. The conductive cellulose substrates with deposited conductive silver contact points are depicted in figure 3.3.

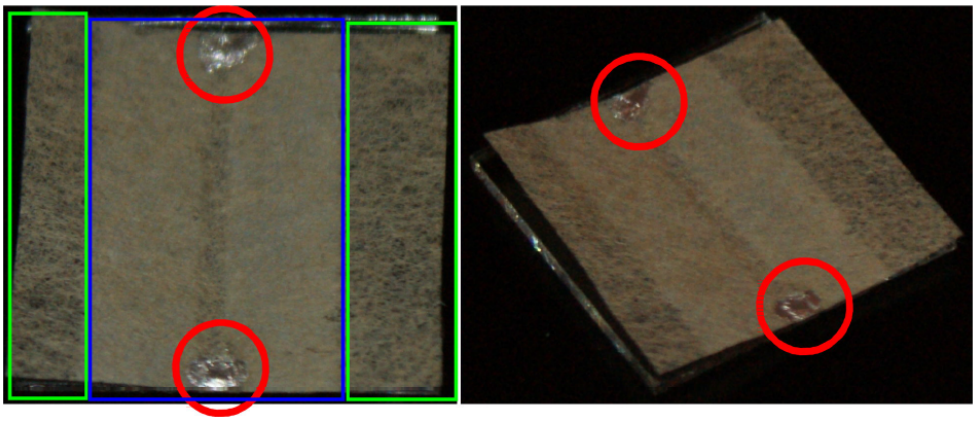

Figure 3.3: "Monopol X" sheets with deposited silver nanowires (blue area), the red circles are showing the conductive silver contact points. The green rectangle is showing the non conductive area of the substrate. [16]

3.1.4 Depositing PEDOT:PSS by drop casting

Before going on with the active layer and to improve wettability of the cellulose substrates and the microscopy slides, they were treated with O_2 plasma for approximately 10 minutes. For detailed parameters see table 3.2. In parallel, the high conductive grade PEDOT:PSS purchased from Sigma-Aldrich was placed in an ultrasonic bath for 30 minutes. After that the cellulose substrates, with the side containing the silver nanowires down, were placed on the microscopy slides and the high conductive grade PEDOT:PSS was consistently applied on the cellulose substrates via drop casting. Such a drop casting process is depicted in figure 3.4. After depositing PEDOT:PSS, the cellulose substrates

Table 3.2: Detailed parameters for the O_2 etching process of the cellulose sheets

parameter	**value**
$Power\ (W)$	100
$t_{etch}\ (min)$	9.5
$p_{etch}\ (mbar)$	0.3
$Flux$	8

were heat treated under argon atmosphere and then put into the glove box. The detailed parameters for the PEDOT:PSS depositing process can be found in table 3.3.

3.1.5 Active layer material preparation

For the active layer solution $P3HT$ and $PC_{60}BM$ were combined in a ratio of 1:2 and dissolved in chlorobenzene. The active layer solution was stirred at 70 $^{\circ}C$ overnight. For the detailed concentrations look at Table 3.4.

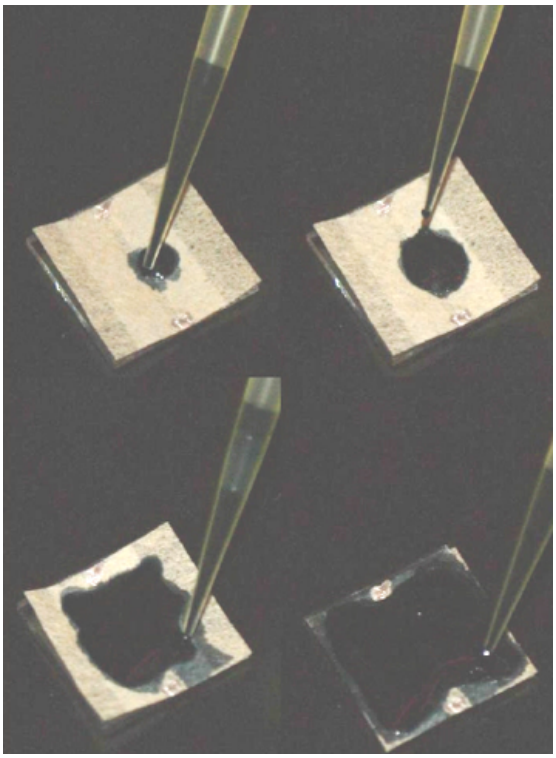

Figure 3.4: Drop casting used as a coating method for depositing PEDOT:PSS [16]

Table 3.3: Detailed parameters for depositing PEDOT:PSS on the cellulose sheets and drying afterwards

parameter	**value**
V_{drop} (μl)	100
T_{dry1} $(^{\circ}C)$	125
t_{dry1} (min)	30
T_{dry2} $(^{\circ}C)$	200
t_{dry2} (min)	30

Table 3.4: Detailed concentrations for the active layer solution

substance	**unit**	**amount**
$P3HT$	mg	50
$PC_{60}BM$	mg	101
Chlorobenzene	ml	3

3.1.6 Depositing active layer material by drop casting

Like the PEDOT:PSS layer, also the active layer solution was uniformly dispersed on the samples via drop casting. But instead of just one layer the active layer solution was spread three times uniformly on the cellulose substrates. After each layer the samples were dried at 70 $^{\circ}C$ for approximately 15 minutes. To look up the detailed parameters for the active layer depositing process see table 3.5. Then the cellulose substrates were transfered to the evaporation glove box.

Table 3.5: Detailed parameters for depositing the active layer on the cellulose sheets and drying afterwards

parameter	**value**
V_{drop1} (μl)	70
T_{dry1} $(^{\circ}C)$	70
t_{dry1} (min)	15
V_{drop2} (μl)	100
T_{dry2} $(^{\circ}C)$	70
t_{dry2} (min)	15
V_{drop3} (μl)	100
T_{dry3} $(^{\circ}C)$	70
t_{dry3} (min)	20

3.1.7 Depositing aluminum as a cathode via thermal evaporation

As a last layer of the organic photovoltaic cell aluminum (Al) was evaporated as a cathode using a thermal evaporator.
The therefore needed thermal evaporator is depicted in figure 3.5. To get a defined structure a shadow mask was used, the shadow mask provides in those defined regions the condensation of the aluminum, the used shadow mask can be seen in figure 3.6. For detailed parameters of the evaporation process see table 3.6. After depositing aluminum the final result and therefore finished organic photovoltaic cell is shown in figure 3.7. In principle the fabricated devices should have now the structure shown in figure 3.8.
So in a short conclusion, as a substrate cellulose sheets were used coated with silver nanowires to make them conductive. Then as another conductive layer PEDOT:PSS was deposited via drop casting. After that $P3HT$ and $PC_{60}BM$

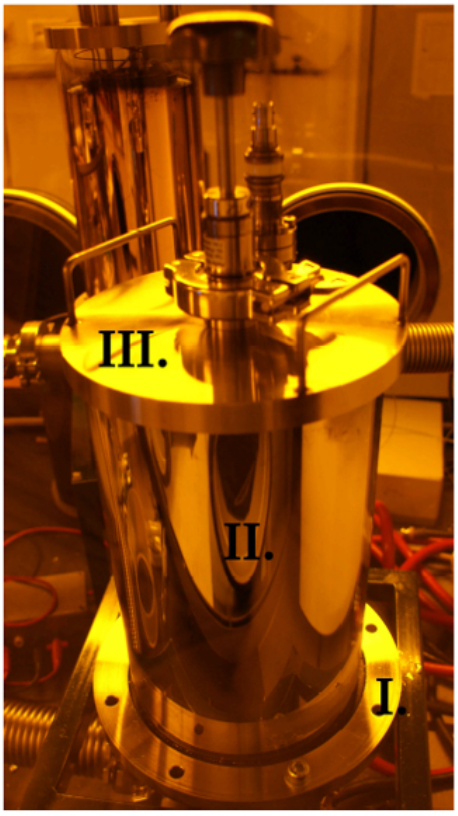

Figure 3.5: Thermal evaporator in the glove box for depositing aluminum [16]

Figure 3.6: Shadowmask used for aluminum evaporation [16]

Table 3.6: Detailed parameters for depositing aluminum on the cellulose sheets as a cathode

parameter	**value**
p_{evap} $(10^{-6} mbar)$	1.5
$EvaporationRate$ (nm/min)	5
d_{Al} (nm)	100

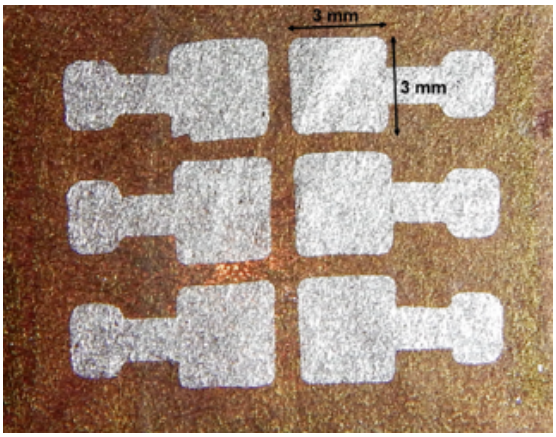

Figure 3.7: Fabricated organic photovoltaic cells based on cellulose substrates [16]

diluted in chlorobenzene were used as the active layer of the device. And in the end aluminum (Al) was evaporated as the upper electrode.

3.2 Results

In this chapter the results of the fabricated organic photovoltaic cells based on cellulose sheets will be presented and discussed. For the characterization of the photovoltaic devices different measurement methods were used. First the resistance of the conductive cellulose substrates was measured, then the transmission spectra for the conductive cellulose substrates were recorded and in the end the current-voltage characteristics of the devices with and without

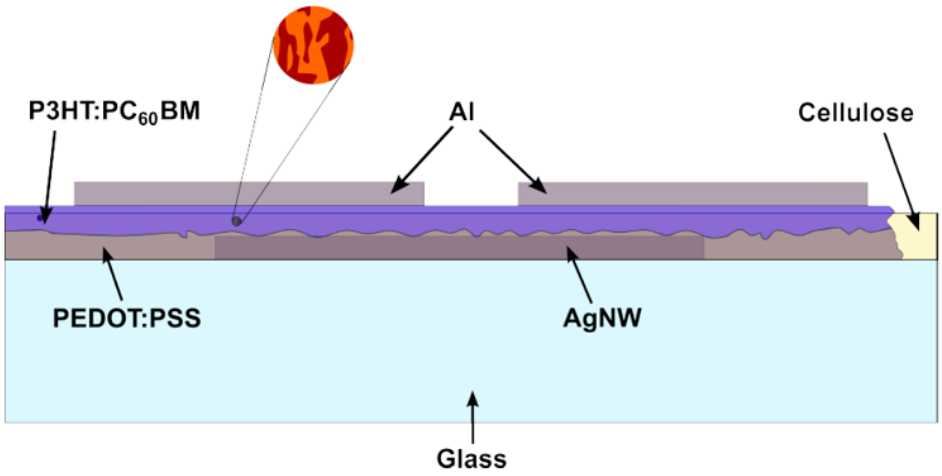

Figure 3.8: Structure of the fabricated device [16]

illumination were measured.

3.2.1 Electrical resistance of the cellulose substrates coated with silver nanowires

After depositing silver nanowires on the cellulose sheets, they become conductive. Therefore the electrical resistance of the coated cellulose sheets was measured with a two probe experiment shown in figure 3.9. The experimental setup is made up of two metal clips fixed in a distance of approximately d = 1 cm and placed on the top of an electrically isolating plastic box. The metal clips were then connected to the Keithley 2602 SourceMeter via triaxial cables. To get the mean electrical resistance each cellulose substrate was measured 3 times, for that the current was measured for a voltage range from -2 V to 2 V. From the recorded curves it was easy to calculate the electrical resistance by simply taking Ohm's law $R = \frac{V}{I}$.

The recorded I-V curves of the first 6 samples (P001-P006) are presented in

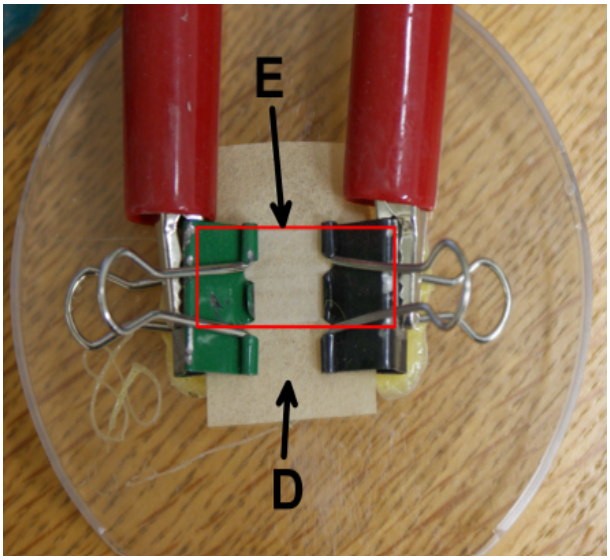

Figure 3.9: Experimental setup for measuring the substrate resistivity (D is the cellulose substrate, E shows the conductive region) [16]

figure 3.10. In the figure can be seen that all curves show ohmic behavior, but the calculated mean resistance of each sample is different, which is depicted in figure 3.11. As one can see quickly for all samples the mean electrical resistance is $< 10\ \Omega$ over a distance of d = 1cm.

For the average electrical resistance of all devices a value of $R_{mean} = 5.47\ \Omega$ was calculated.

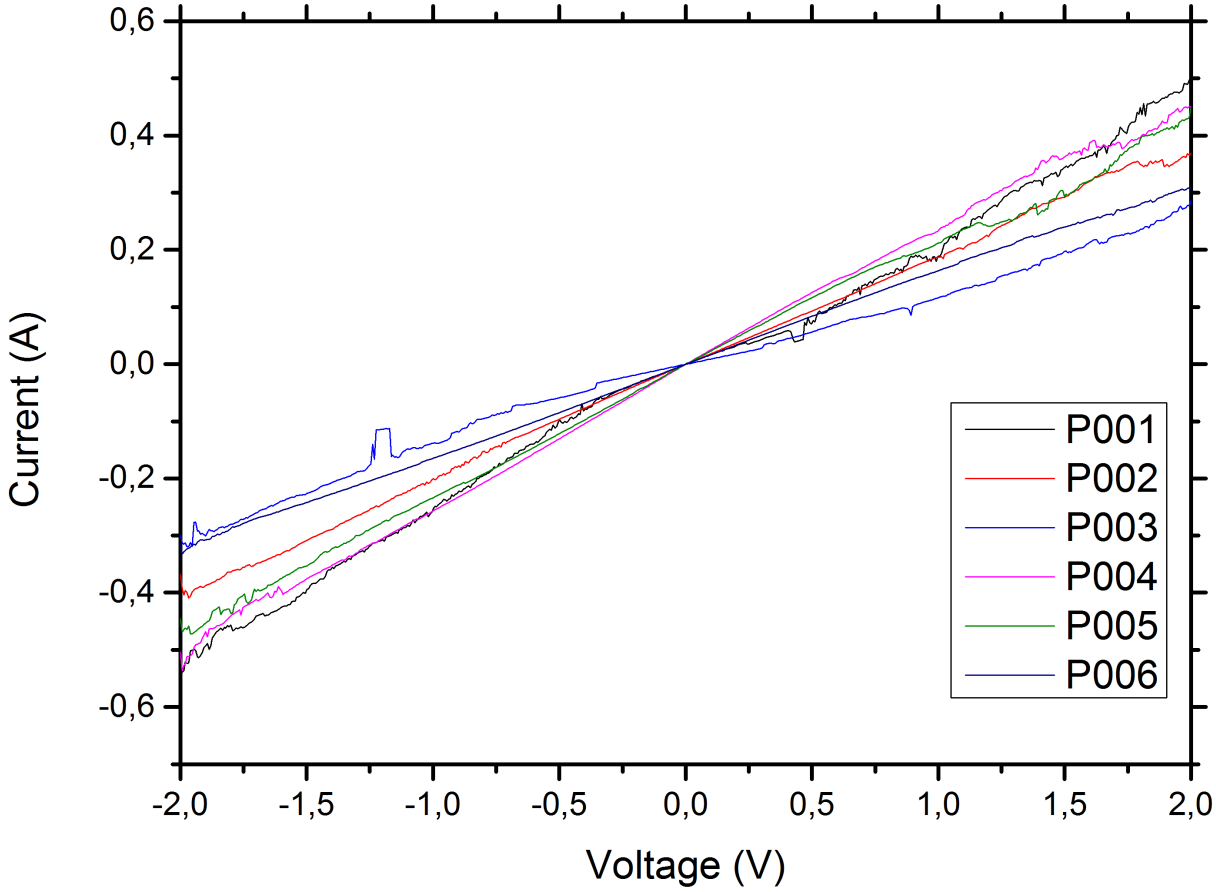

Figure 3.10: Current-Voltage (I-V) characteristics for the cellulose substrates coated with silver nanowires

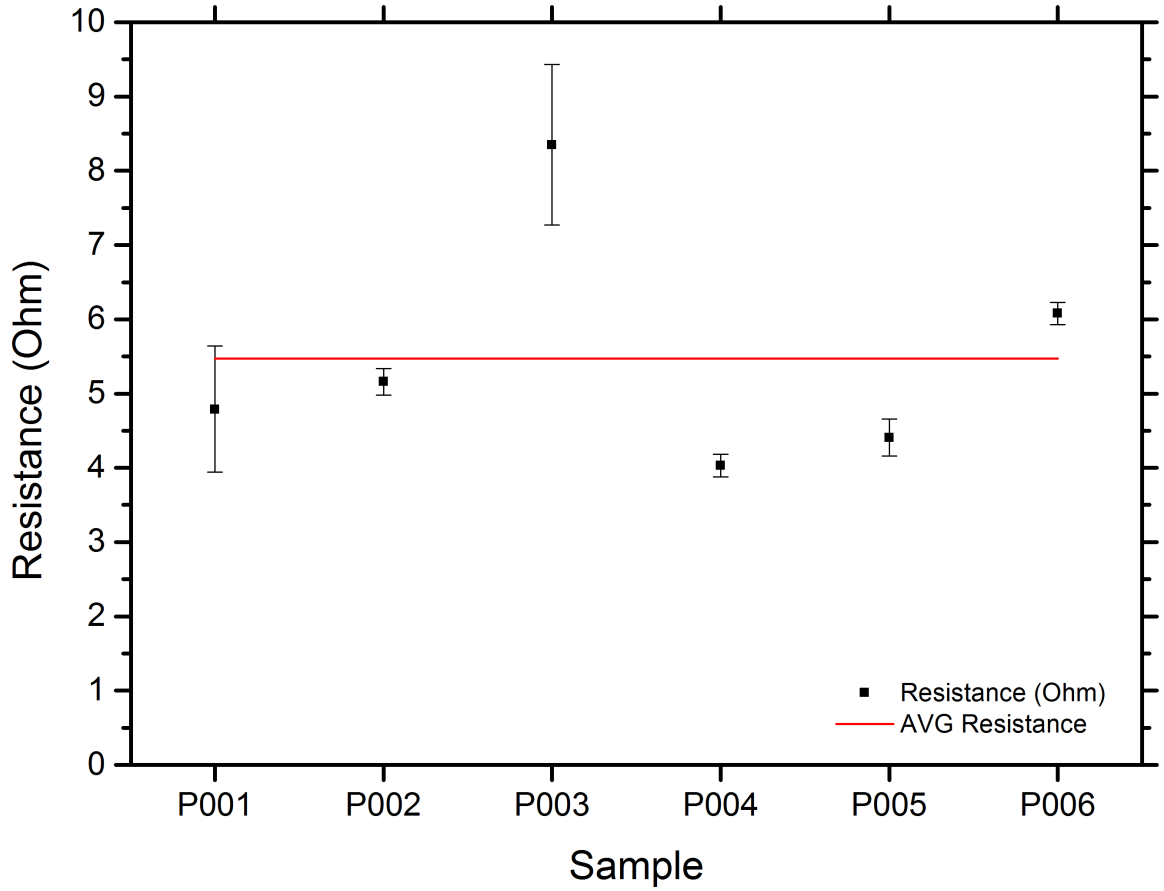

Figure 3.11: Average Resistance per cellulose substrate coated with silver nanowires and the overall average resistance

3.2.2 Transmission of the cellulose substrates coated with silver nanowires

To measure the transmission for the substrates a SHIMADZU UV spectrophotometer depicted in figure 3.12 was used. Therefore the cellulose substrates coated with silver nanowires were measured relative to untreated cellulose substrates, the result is shown in figure 3.13.

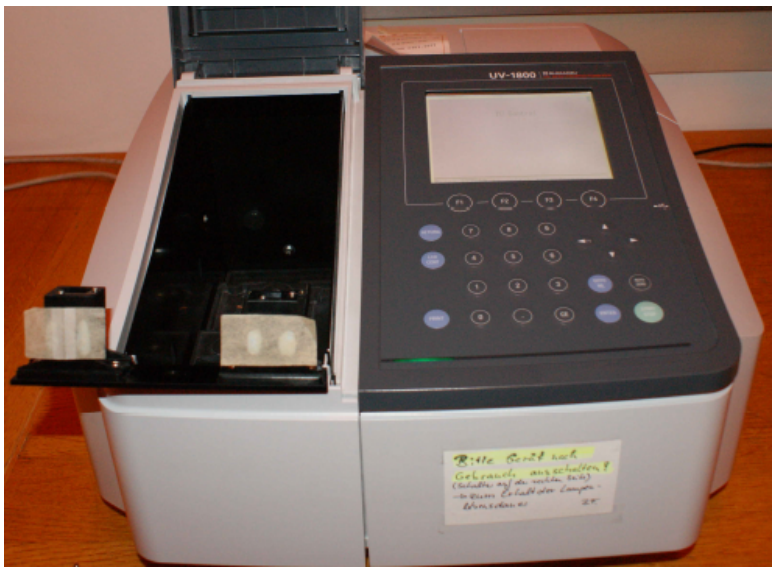

Figure 3.12: SHIMADZU UV Spectrophotometer UV 1800 [16]

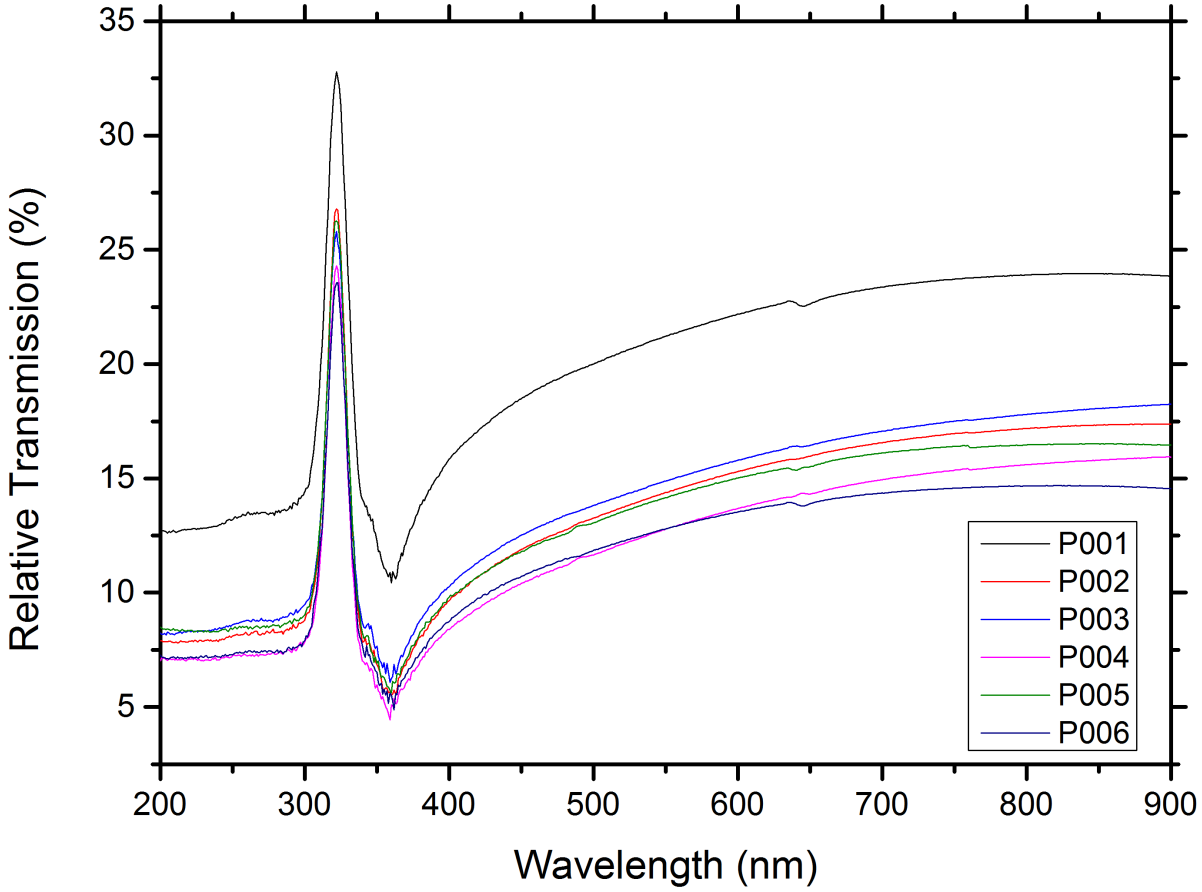

Figure 3.13: Transmission spectra for the different cellulose substrates coated with silver nanowires

As can be seen over a broad region for wavelengths longer than 450 nm the transmission spectra shows nearly constant performance. The main reason for the reduction in transmission is the reflection behavior of the dip-coated silver nanowires [31]. For wavelengths smaller than 450 nm the predominant effect is plasmon absorption, which has its maximum at approximately 360 nm where it leads to a minimum in transmission. Another side effect of the plasmon absorption is the grayish manifestation of the dip-coated silver nanowires [16, 31, 32]. The peak at around 320 nm is caused by a light source change of the spectrophotometer and can thus be ignored [16].
The withdrawal speed in the dip coating process was $v_{wd} = 0.25mm/min$, so it is comparable to the black line from Heribert Kopeinik fabrication process shown in figure 3.14[16]. The thicker the silver nanowire coating, the higher is the reflectivity, which means a decrease of withdrawal speed leads to decreasing transmittance.
By comparing the results with the results from Kopeinik, it can be seen that the relative transmission from our cellulose substrates is lower than for Kopeiniks devices. That is because Kopeinik has diluted his silver nanowires with isopropanol, but without stating the quantity of isopropanol, so the silver nanowires in our attempt have a greater density, which leads to lower transmission. But it is still enough transmission to have a working organic photovoltaic cell, which can be seen at the characteristics for the fabricated organic photovoltaic cells.

3.2.3 Characteristics of the fabricated organic photovoltaic cells based on cellulose sheets

To observe the characteristics of the fabricated organic photovoltaic devices, the cells have been measured two times. For this purpose a variable voltage

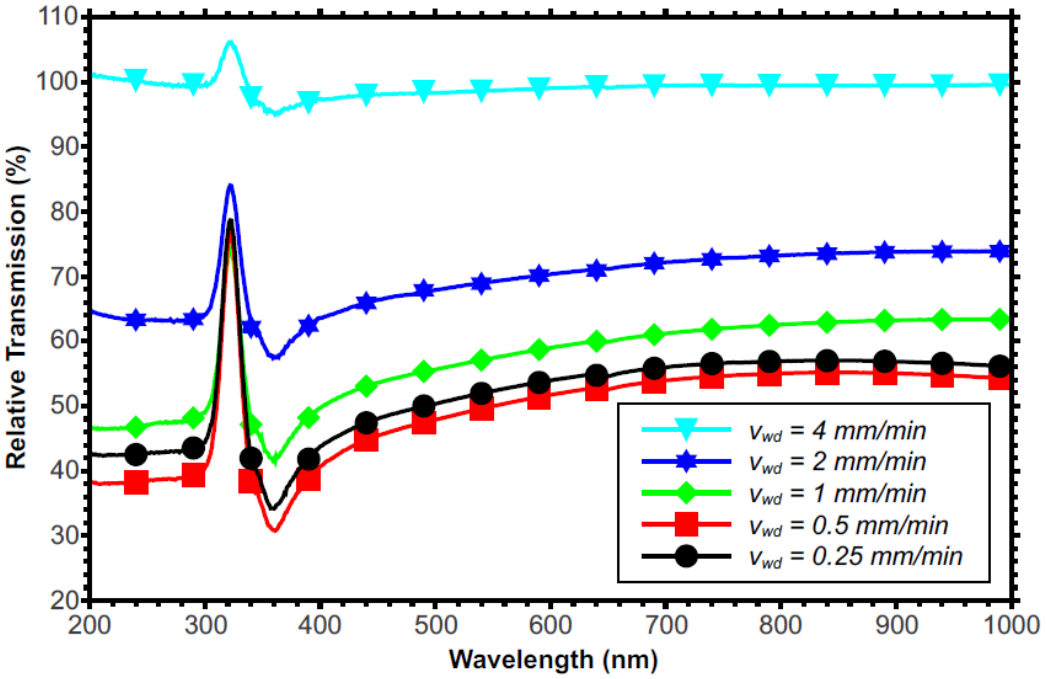

Figure 3.14: Transmission spectra from Heribert for AgNW coated cellulose substrates with different withdrawal speeds. [16]

was applied to the tested photovoltaic device and then the photocurrent was measured for each value. The applying of the voltage and the measurement of the photocurrent was performed using a Keithley 2602 SourceMeter, which was controlled by a computer with the program *TSPExpress*. The experimental setup is depicted in figure 3.15.

First the measurement was done in the dark, therefore the samples were cov-

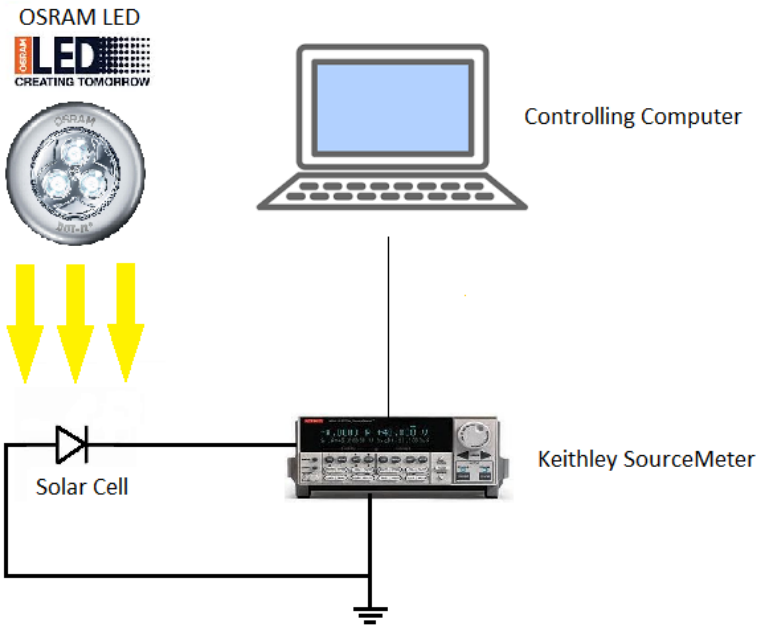

Figure 3.15: Experimental setup for J-V characterization

ered with an optically opaque cloth. A picture was taken and can be seen in figure 3.16, in this figure the measurement apparatus is shown in ambient light, but this was just for taking the photo.

After measuring the samples in the dark, the next step was to illuminate them and then do the measurements again. For lighting the samples a LED from the company OSRAM was used. The measurement setup for doing the characterization under illumination is depicted in figure 3.17. So as a result the

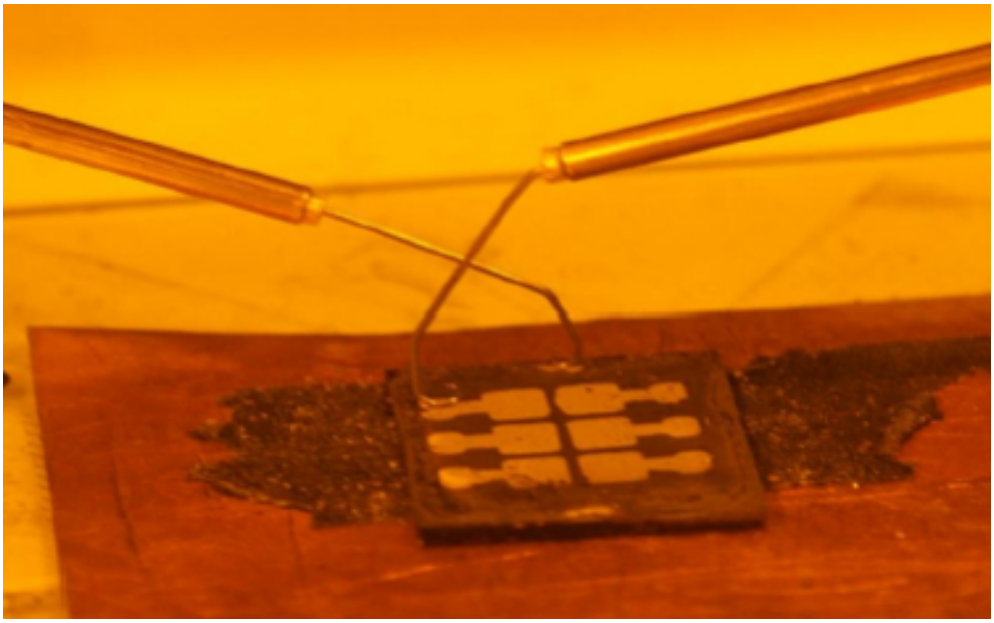

Figure 3.16: Measurement method for J-V characterization under yellow light (just for the figure) [16]

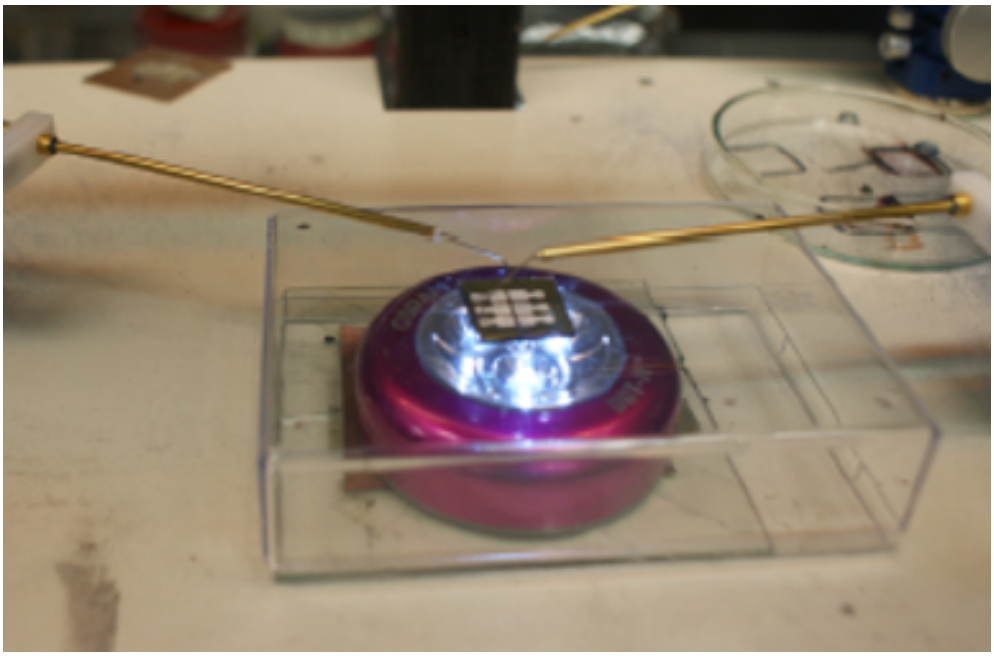

Figure 3.17: Measurement method for J-V characterization under LED illumination [16]

characteristics of two working photovoltaic cells based on cellulose sheets will now be presented, first the samples $P102\_2$ and $P004\_4$ will be called "paper1" and "paper2" in this master thesis for better readability.

The current density-voltage characteristics for the fabricated organic photovoltaic cell "paper1" are shown linear in figure 3.18, the characteristics were also plotted in semi-log scale, which is depicted in figure 3.19. The black line always presents the measurement recorded under dark conditions, while the red line was recorded under LED irradiation. So what can be seen immediately is, that the two plotted lines (dark, illuminated) are shifted on the x-axis (figure 3.19), which basically means that there is a photocurrent available and the photovoltaic cell is working. It is also possible to read off the figure 3.20 that for the fabricated device "paper1" the photocurrent gets 10 times bigger under direct illumination than under dark conditions.

To obtain the open-circuit voltage V_{OC} and the short-circuit current density J_{SC} it is easier to look at the semilogarithmic plot (figure 3.19). Under direct lighting it was found that the organic photovoltaic device "paper1" has a open-circuit voltage of V_{OC} = 0.40 V and a short-circuit current density of J_{SC} = 1.03 $\frac{mA}{cm^2}$.

To observe the fill factor of the fabricated device, the maximum power point (MPP) was needed. Therefore, the power-voltage characteristics were plotted in figure 3.21 and the highest point in the plot is the MPP. The organic photovoltaic cell "paper1" showed a maximum power point of V_{MPP} = 0.23 V and J_{MPP} = 0.65 $\frac{mA}{cm^2}$. The fill factor of the device was now observed with FF = $\frac{V_{MPP} \cdot J_{MPP}}{V_{OC} \cdot J_{SC}}$ = 36.2 %.

The collected results of the fabricated organic photovoltaic cell "paper1" can be looked up in table 3.7.

Table 3.7: Collected results from the characteristics of "paper1"

Measure	**Measure description**	**Value**	**Unit**
J_{SC}	short-circuit current density	1.03	$\frac{mA}{cm^2}$
V_{OC}	open-circuit voltage	0.40	V
J_{MPP}	maximum power point current density	0.647	$\frac{mA}{cm^2}$
V_{MPP}	maximum power point voltage	0.2304	V
FF	Fill Factor	36.2	%

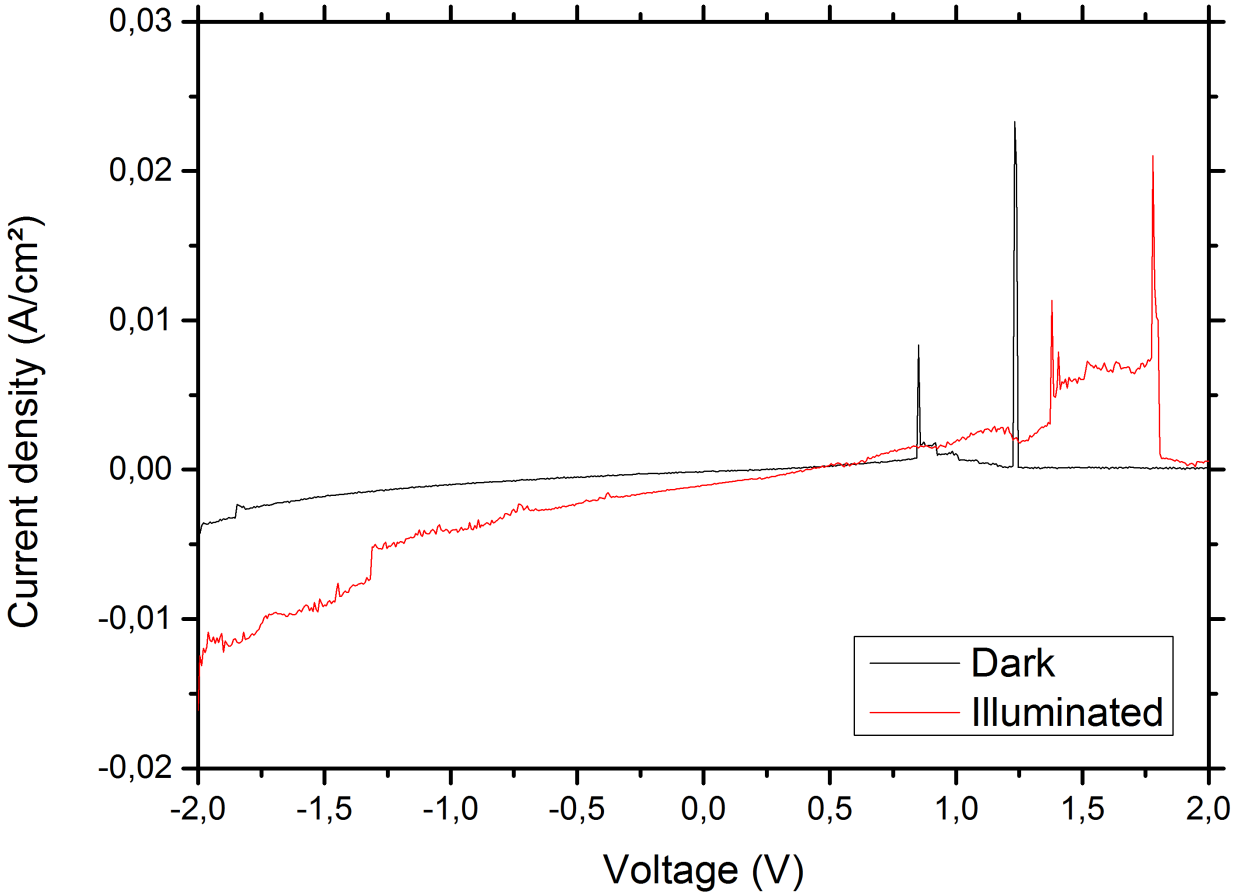

Figure 3.18: Current density-Voltage (J-V) characteristics for fabricated organic photovoltaic cell ”paper1”

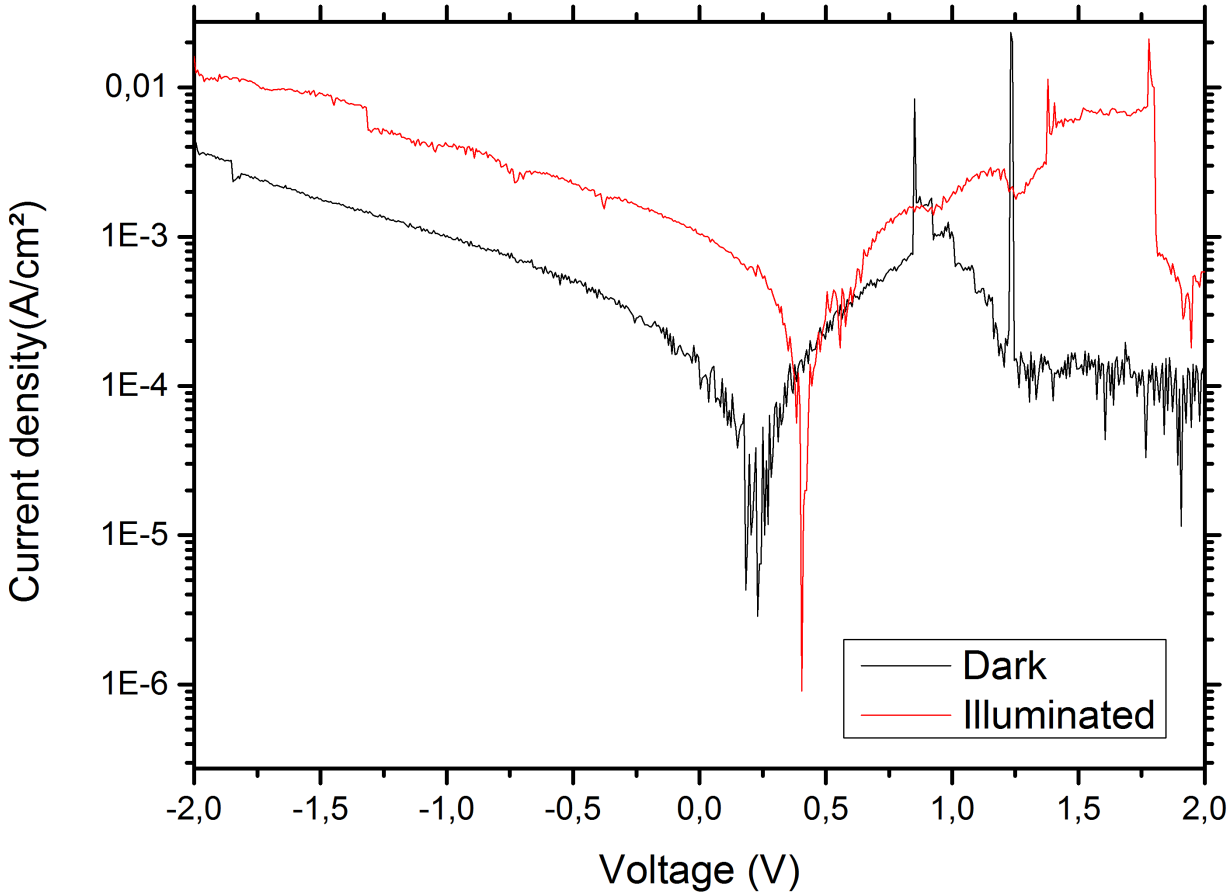

Figure 3.19: Logarithmic J-V-characteristics for fabricated organic photovoltaic cell ”paper1”

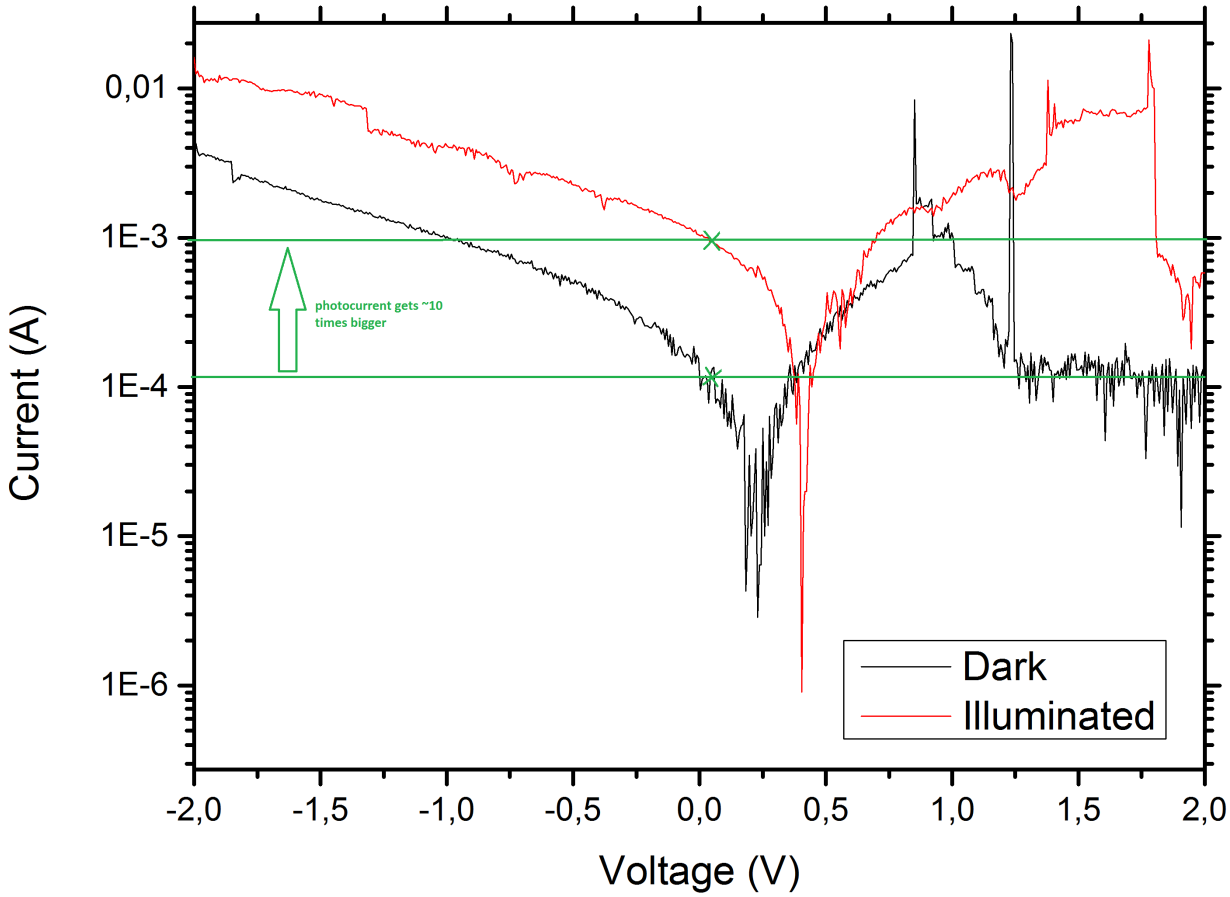

Figure 3.20: Logarithmic J-V-characteristics with comparison of the photocurrent for fabricated organic photovoltaic cell "paper1"

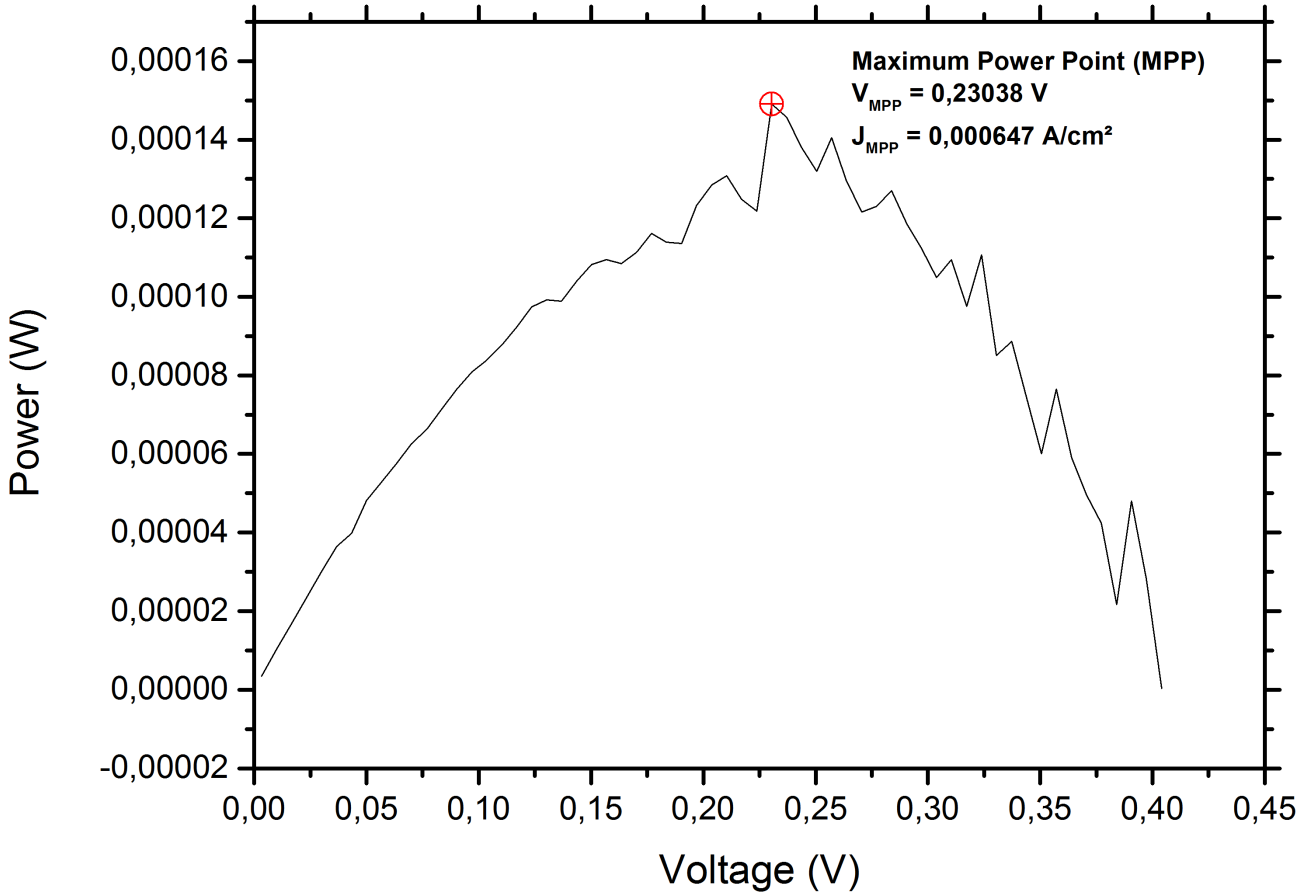

Figure 3.21: Power-Voltage (P-V) characteristics for fabricated organic photovoltaic cell ”paper1” to get MPP

As well as previously in "paper1", the current density-voltage characteristics for the fabricated organic photovoltaic cell "paper2" are shown in semi-log scale in figure 3.22. The black line presents as above the measurement recorded under dark conditions, while the red line was recorded under LED irradiation. So what can be seen again immediately is, that the two plotted lines (dark, illuminated) are also shifted on the x-axis (figure 3.22), which basically means that there is a photocurrent available and the photovoltaic cell is working. It is also possible to read off the figure 3.22 that for the fabricated device "paper2" the photocurrent gets not so much bigger (only approximately 2 times) under direct illumination than under dark conditions.

To obtain the open-circuit voltage V_{OC} and the short-circuit current density J_{SC} it is easier to look at the semilogarithmic plot (figure 3.22). Under direct lighting it was found that the organic photovoltaic device "paper2" has a open-circuit voltage of V_{OC} = 0.29 V and a short-circuit current density of J_{SC} = 0.517 $\frac{mA}{cm^2}$.

To observe the fill factor of the fabricated device, the maximum power point (MPP) was needed. Therefore the power-voltage characteristics were plotted in figure 3.21 and the highest point in the plot is the MPP. The organic photovoltaic cell "paper2" showed a maximum power point of V_{MPP} = 0.21 V and J_{MPP} = 0.151 $\frac{mA}{cm^2}$. The fill factor of the device was now observed with FF = $\frac{V_{MPP} \cdot J_{MPP}}{V_{OC} \cdot J_{SC}}$ = 36.5 %.

The collected results of the fabricated organic photovoltaic cell "paper2" can be looked up in table 3.8.

Table 3.8: Collected results from the characteristics of "paper2"

Measure	**Measure description**	**Value**	**Unit**
J_{SC}	short-circuit current density	0.517	$\frac{mA}{cm^2}$
V_{OC}	open-circuit voltage	0.29	V
J_{MPP}	maximum power point current density	0.151	$\frac{mA}{cm^2}$
V_{MPP}	maximum power point voltage	0.21	V
FF	Fill Factor	36.5	%

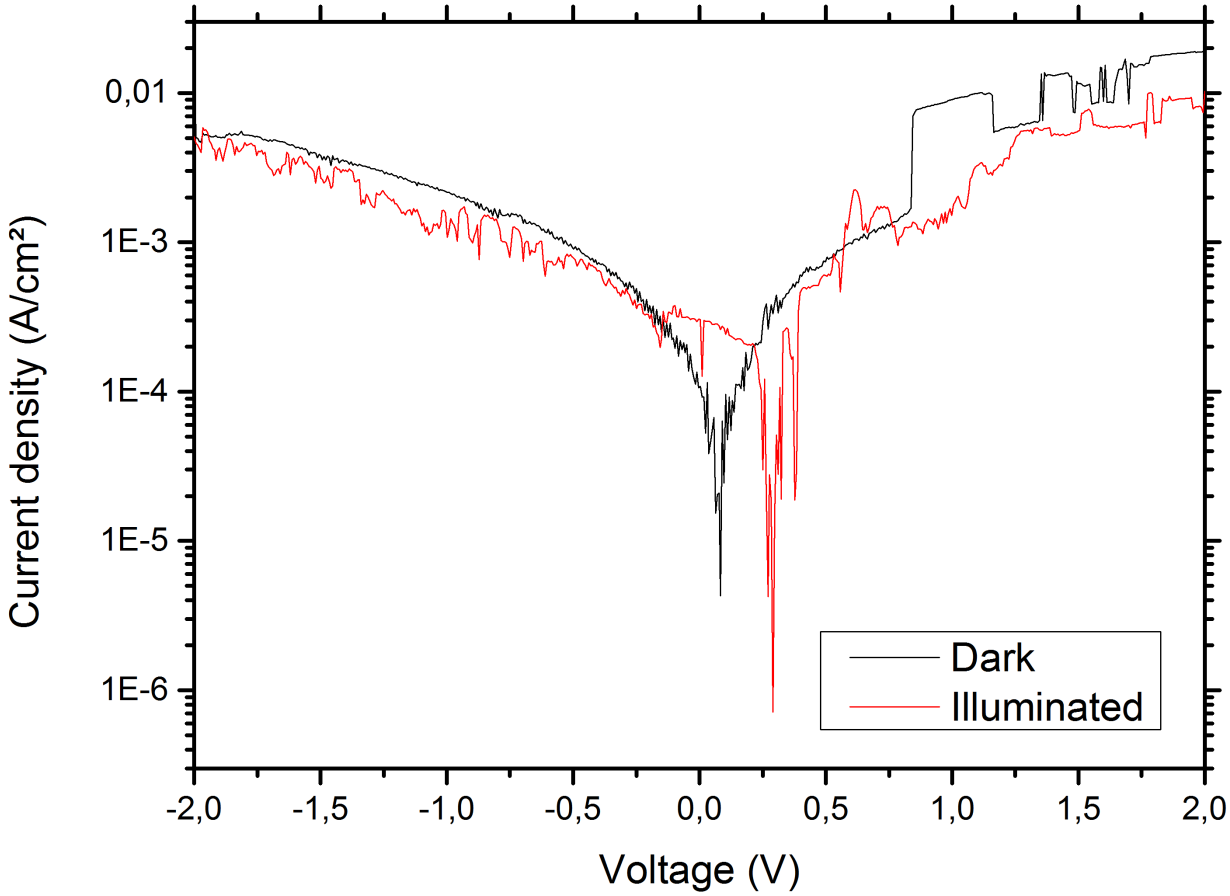

Figure 3.22: Logarithmic J-V-characteristics for fabricated organic photovoltaic cell ”paper2”

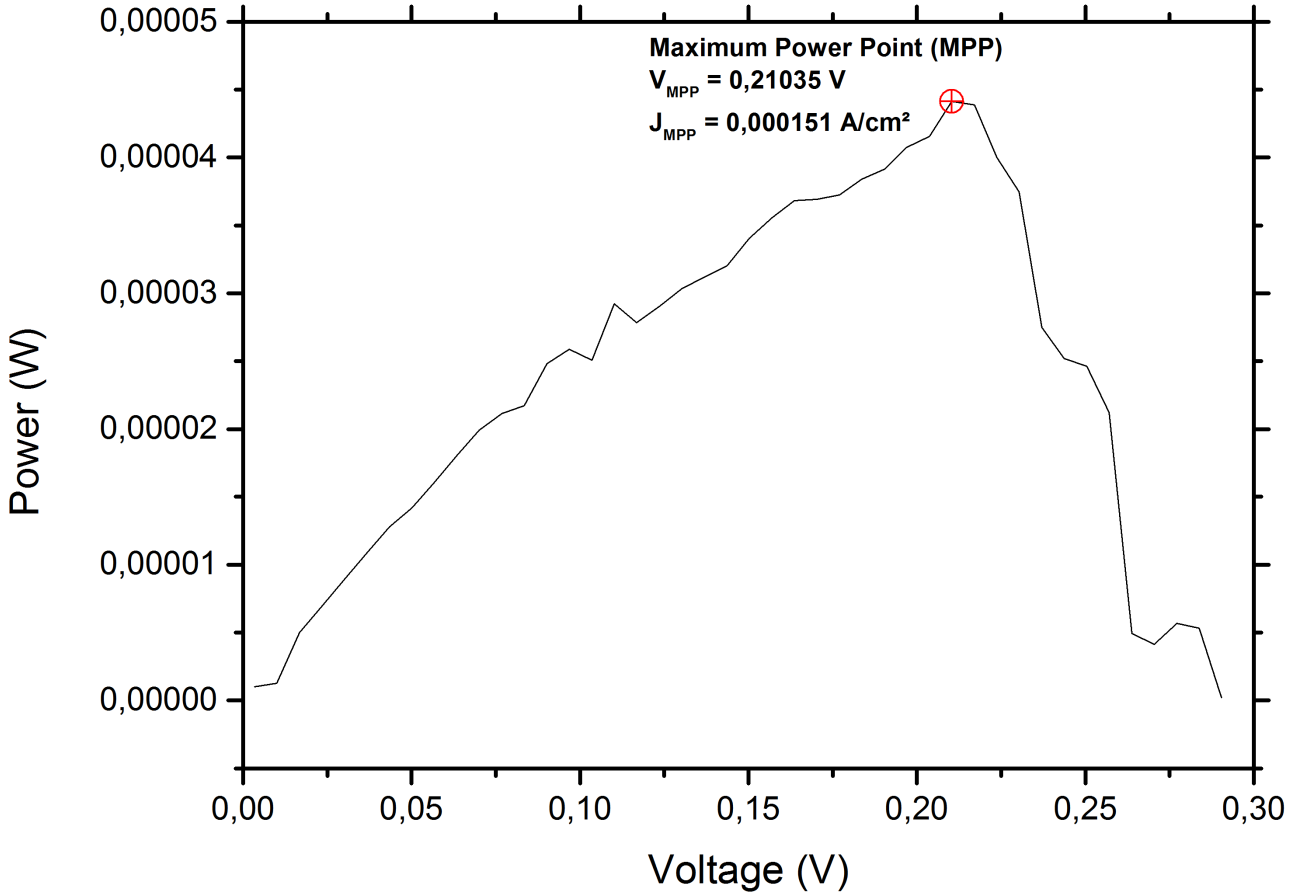

Figure 3.23: Power-Voltage (P-V) characteristics for fabricated organic photovoltaic cell ”paper2”

4 Organic photovoltaic cells based on cellulose fibers

4.1 Fabrication process

In this chapter the fabrication process for an organic photovoltaic cell based on viscose cellulose fibers will be presented. To have a better overview, the whole fabrication process was depicted in a flowchart (Figure 4.1).

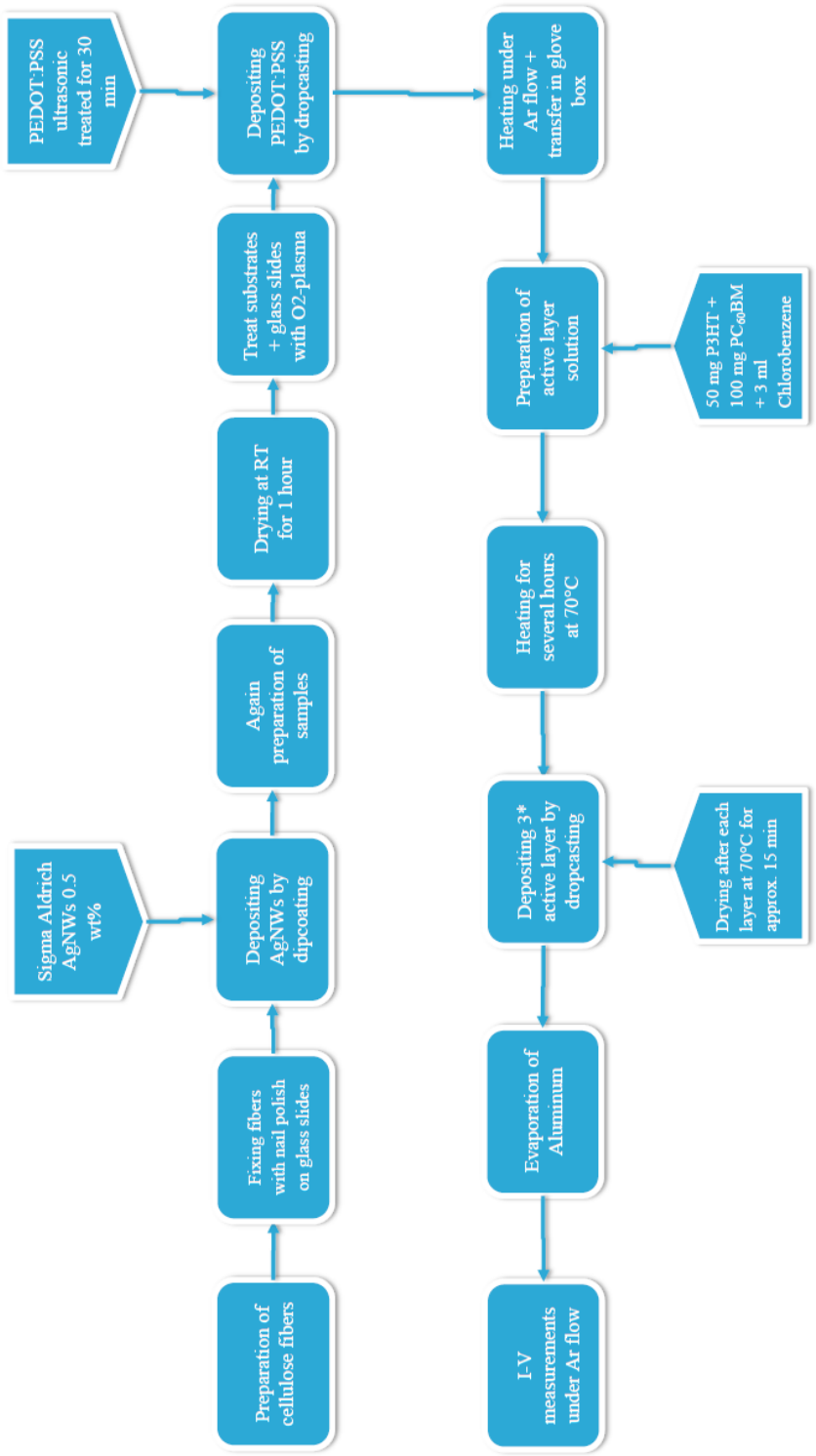

Figure 4.1: Flowchart for the fabrication process of the cellulose fibers

The principal structure of the photovoltaic fibers was as follows (Figure 4.2): The viscose fiber is first dip coated with silver nanowires as a flexible inner electrode. The next layer is the organic absorbing layer ($PEDOT$:PSS + $P3HT$:$PC_{60}BM$) of the flexible photovoltaic device. This layer is applied via drop casting. The final layer is the external transparent electrode. This is the only layer that has not been made by dip coating/drop casting in the proof of principle device shown in this master thesis.

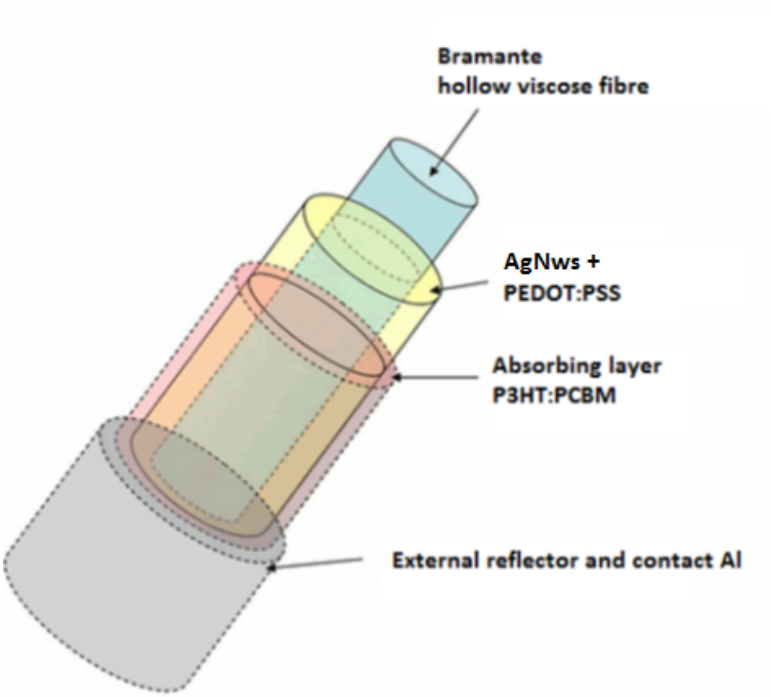

Figure 4.2: Structure of the photovoltaic cells based on cellulose fibers

4.1.1 Preparation of the cellulose fibers

As a substrate hollow regenerated cellulose fibers with a diameter of 2.1 dtex (about 20 μm) and a length of about 4 cm were used. The fibers were supplied

by Kelheim Fibres GmbH, Kelheim, Germany. A scanning electron microscope (SEM) image of the bramante hollow viscose fiber is depicted in figure 4.3, in which one can easily see that the fibers are segmented. The segments are an additional advantage in the device build in this work, as the segments cannot be penetrated by the dip coating solutions. Therefore, dip coating of the fibers resulted only in coatings on the outside of the fibers and not on the inside of the fibers [33]. As with the cellulose sheets it was also tried for better

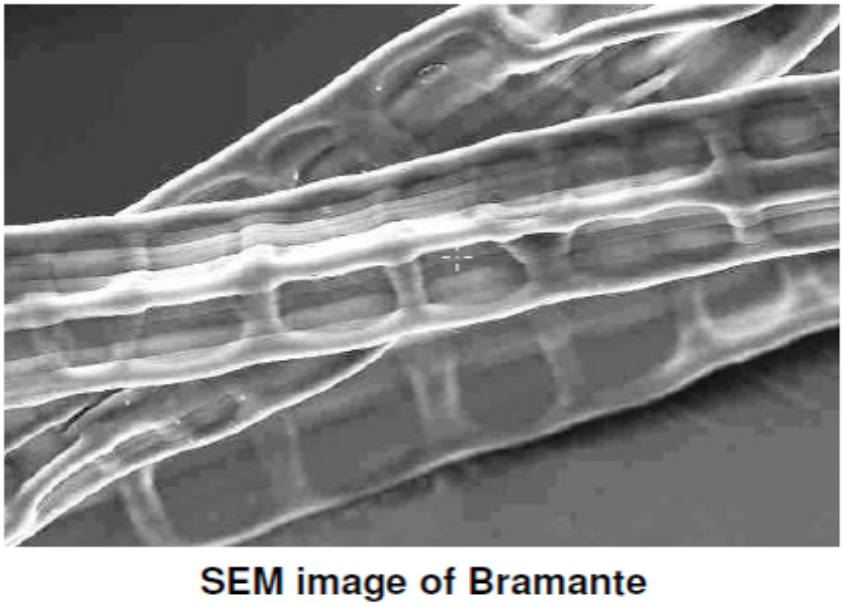

Figure 4.3: SEM image of a bramante hollow viscose fibre [33]

handling to apply the viscose fibers on glass slides. So the first try was to do it exactly like for the sheets, but it did not work because the fibers were only swimming on the surface in the dip-coating process and not sinking. So the next try was done like it can be seen in figure 4.4, but here the problem was, that the fibers were stuck on the glass. Those two problems were only a part of the problems in the fabrications process, but in the end a working construction has been found like in figure 4.5. The fibers were fixed using customary nail polish, because it was shown previously that super glue tends to form a coat

on cellulose fibers [34]. Finally with this structure also the dip-coating process was working (see Figure 4.6).

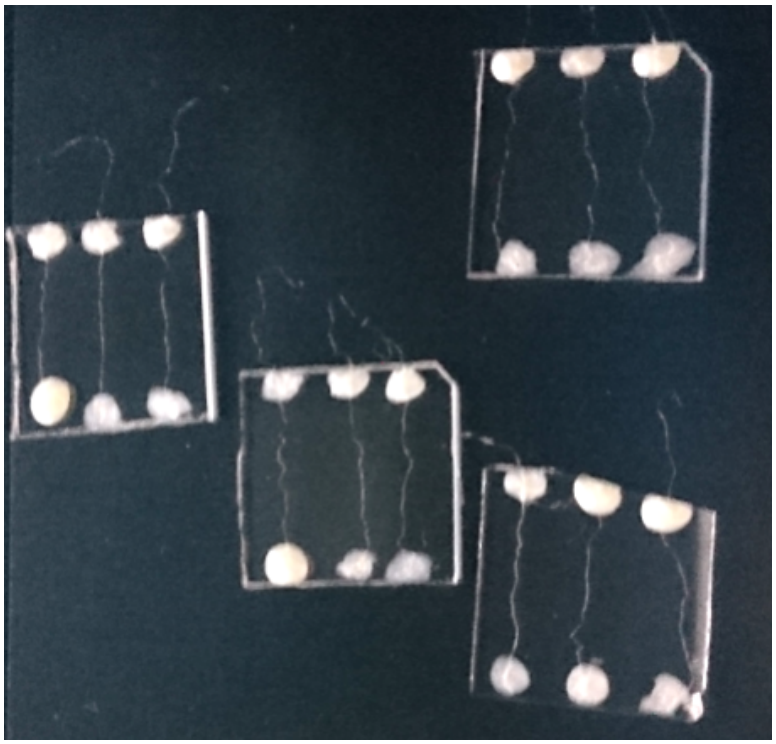

Figure 4.4: First try of manufacturing an organic photovoltaic fiber

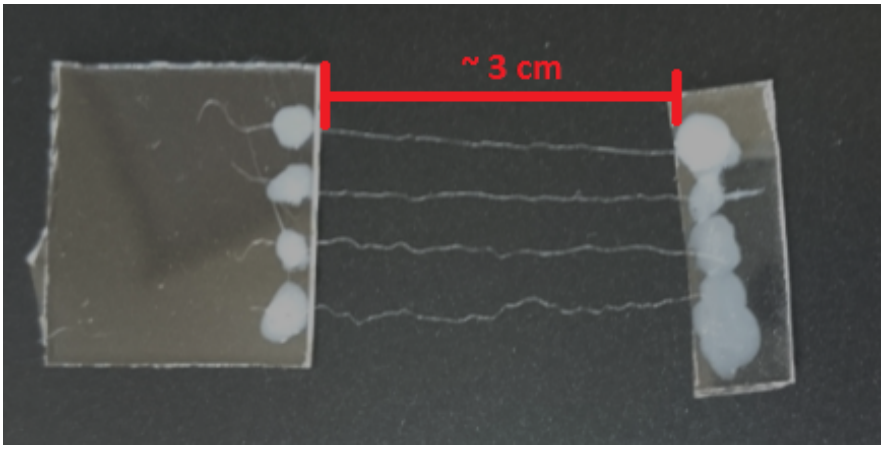

Figure 4.5: Working construction for dip-coating the cellulose fiber

4.1.2 Depositing silver nanowires by dip coating

Past preparation of the viscose fibers, electrically conductive cellulose fibers were established using silver nanowires as a conductive layer. There a suspension of silver nanowires (diameter: 115 nm, length: 20 - 50 μm) in isopropanol supplied by Sigma-Aldrich was used. The inner electrode on the cellulose fiber surface was made by dip coating the fibers in this supplied suspension. As a dip coater the SDI Nano DIP ND-0407 dip-coater was used (see figure4.6). After the dip coating process the now conductive fibers were dried at room temperature for 1 hour. The detailed parameters for the dip coating process of the fibers can be found in table 4.1.

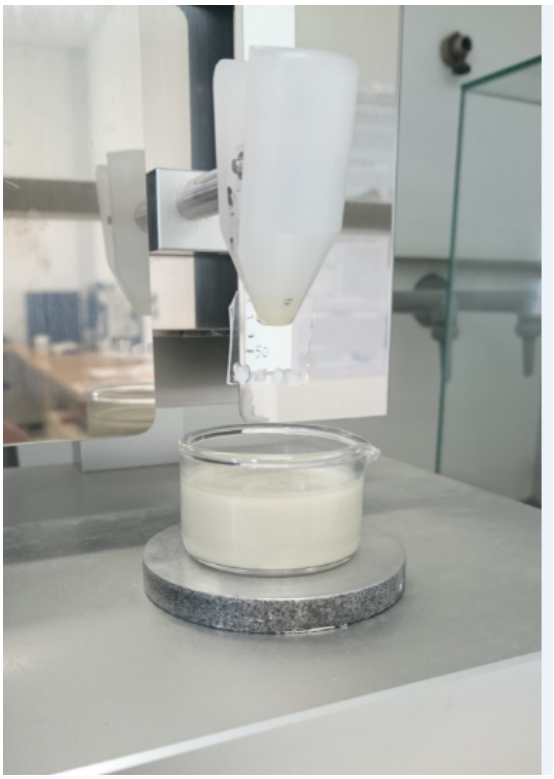

Figure 4.6: Depositing silver nanowires on the cellulose fibers by dip-coating

Table 4.1: Detailed parameters for the dip coating process of the viscose fibers

parameter	value
v_{dip} $(\mu m/s)$	500
t_{stop} (s)	30
v_{wd} $(\mu m/s)$	33.33

4.1.3 Preparation of the conductive cellulose fibers

After depositing silver nanowires on the cellulose fibers, on the end of the fibers conductive silver contact points were set to link the anode after fabrication for making I-V characterization of the organic photovoltaic cells. The conductive silver contact points need to dry at room temperature for about 1 hour.

Before going on with the active layer and to improve wettability of the cellulose fibers and the microscopy slides, they were treated with O_2 plasma for approximately 10 minutes. For detailed parameters see table 4.2.

Table 4.2: Detailed parameters for the O_2 etching process of the viscose fibers

parameter	value
$Power$ (W)	100
t_{etch} (min)	9.5
p_{etch} $(mbar)$	0.3
$Flux$	8

4.1.4 Depositing PEDOT:PSS by drop casting

In parallel to the etching process, the high conductive grade PEDOT:PSS purchased from Sigma-Aldrich was placed in an ultrasonic bath for 30 minutes.

After that the high conductive grade PEDOT:PSS was consistently applied on the cellulose fibers via drop casting.
After depositing PEDOT:PSS, the cellulose substrates were heat treated under Ar atmosphere and then put into the chemical glove box.The detailed parameters for the PEDOT:PSS depositing process can be found in table 4.3.

Table 4.3: Detailed parameters for depositing PEDOT:PSS on the cellulose fibers and drying afterwards

parameter	**value**
V_{drop} (μl)	100
T_{dry1} $(^{\circ}C)$	125
t_{dry1} (min)	30
T_{dry2} $(^{\circ}C)$	200
t_{dry2} (min)	30

4.1.5 Active layer material preparation

For the active layer solution $P3HT$ and $PC_{60}BM$ were combined in a ratio of 1:2 and dissolved in chlorobenzene. The active layer solution was stirred at 70 $^{\circ}C$ overnight. For the detailed concentrations look at Table 4.4.

Table 4.4: Detailed concentrations for the active layer solution

substance	**unit**	**amount**
$P3HT$	mg	50
$PC_{60}BM$	mg	100
$Chlorobenzene$	ml	3

4.1.6 Depositing active layer material by drop casting

Like the PEDOT:PSS layer, also the active layer solution was uniformly dispersed on the samples via drop casting. But instead of just one layer the active layer solution was spread three times uniformly on the cellulose fibers. After each layer the samples were dried at 70 $^{\circ}C$ for approximately 15 minutes. To look up the detailed parameters for the active layer depositing process see table 4.5. Afterwards the cellulose fibers were transfered to the evaporation glove box.

Table 4.5: Detailed parameters for depositing the active layer on the cellulose fibers and drying afterwards

parameter	**value**
V_{drop1} (μl)	70
T_{dry1} $(^{\circ}C)$	70
t_{dry1} (min)	15
V_{drop2} (μl)	100
T_{dry2} $(^{\circ}C)$	70
t_{dry2} (min)	15
V_{drop3} (μl)	100
T_{dry3} $(^{\circ}C)$	70
t_{dry3} (min)	20

4.1.7 Depositing aluminum as a cathode via thermal evaporation

As a last layer of the organic photovoltaic cell aluminum (Al) was evaporated as a cathode using a thermal evaporator.

The therefore needed thermal evaporator is depicted in figure 3.5. To get a defined structure a slit shadow mask was used, the shadow mask provides in those defined regions the condensation of the aluminum. For detailed parameters of the evaporation process see table 4.6. In principle the fabricated

Table 4.6: Detailed parameters for depositing aluminum on the cellulose fibers as a cathode

parameter	**value**
p_{evap} $(10^{-6} mbar)$	2.0
$EvaporationRate$ (nm/min)	8
d_{Al} (nm)	100

devices should have now the structure shown in figure 4.7.
So in a short conclusion, as a substrate bramante cellulose fibers were used coated with silver nanowires to make them conductive. Then as another conductive layer PEDOT:PSS was deposited via drop casting. After that $P3HT$ and $PC_{60}BM$ diluted in chlorobenzene were used as the active layer of the device. And in the end aluminum (Al) was evaporated as the upper electrode. In the area where aluminum was coated, the fibers were no longer flexible, but stiff.

4.2 Results

In this chapter the results of the fabricated organic photovoltaic cells based on cellulose fibers will be presented and discussed. For the characterization of the photovoltaic devices different measurement methods were used. First the resistance of the conductive cellulose substrates was measured and then the current-voltage characteristics of the devices with and without illumination were measured.

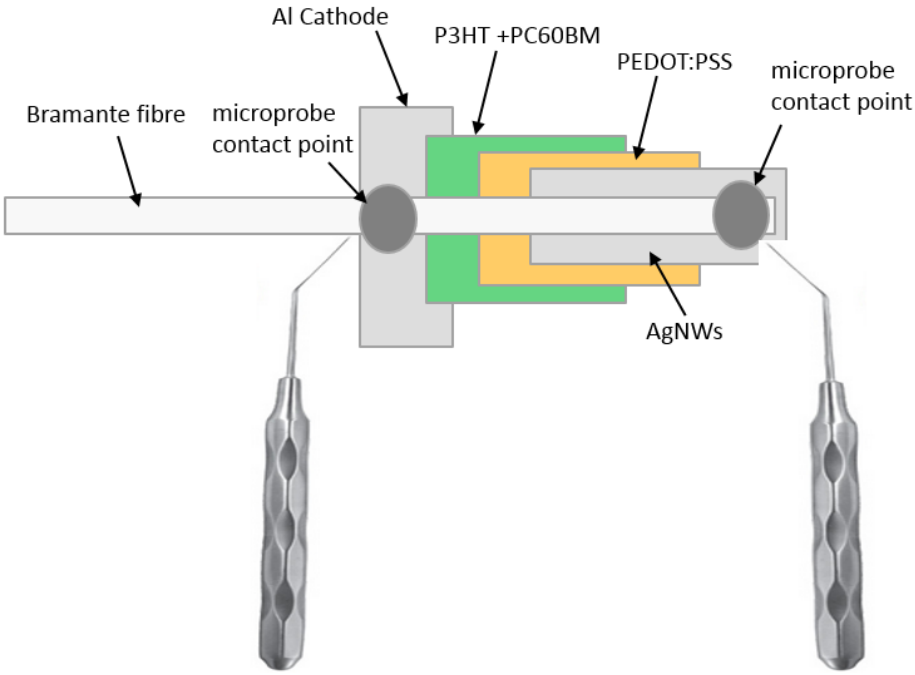

Figure 4.7: Cross-section of a fabricated organic photovoltaic fiber with the contact points for the micro probes

4.2.1 Electrical resistance of the cellulose fibers coated with silver nanowires

After depositing silver nanowires on the cellulose fibers, they become conductive. Therefore the electrical resistance of the coated cellulose sheets was measured with a two probe experiment. The experimental setup is made up of two microprobes fixed in a distance of d = 1 cm and placed on the top of an electrically isolating plastic box. The microprobes were then connected to the Keithley 2602 SourceMeter via triaxial cables.
To get the mean electrical resistance 11 cellulose fibers were measured, for that the current was measured for a voltage range from -1 V to 1 V. From the recorded curves it was easy to calculate the electrical resistance by simply taking Ohm's law $R = \frac{V}{I}$.
The recorded I-V curves of one cellulose fiber is presented in figure 4.8. In the figure it can be seen that the curve has ideal ohmic behavior. For the average electrical resistance of all 11 fibers a value from R_{mean} = 45 Ω was calculated.

4.2.2 Characteristics of the fabricated organic photovoltaic cells based on cellulose sheets

To observe the characteristics of the fabricated organic photovoltaic devices, the cells have been measured two times. For this purpose a variable voltage was applied to the tested photovoltaic device and then the photocurrent was measured for each value. The applying of the voltage and the measurement of the photocurrent was performed using a Keithley 2602 SourceMeter, which was controlled by a computer with the program $TSPExpress$. The experimental setup is depicted in figure 3.15.

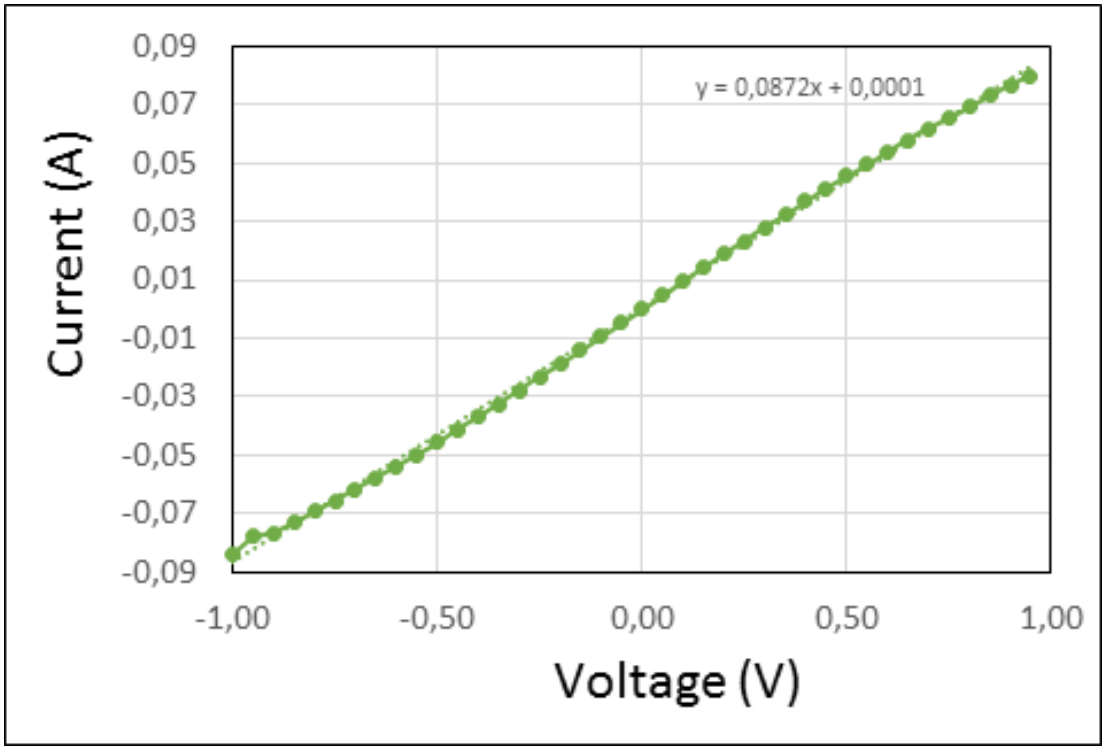

Figure 4.8: Current-Voltage (I-V) characteristics for a cellulose fiber coated with silver nanowires

First the measurement was done in the dark, therefore the samples were covered with an optically opaque cloth. A picture was taken and can be seen in figure 3.16, in this figure the measurement apparatus is shown in ambient light, but this was just for taking the photo. After measuring the samples in the dark, the next step was to illuminate them and then do the measurements again. For lighting the samples a LED from the company OSRAM was used. The measurement setup for doing the characterization under illumination is depicted in figure 3.17.

So as a result the characteristics of two working photovoltaic cells based on cellulose fibers will now be presented, first the samples $P162\_1$ and $P203\_2$ will be called "fiber1" and "fiber2" in the master thesis for better readability.

The current density-voltage characteristics for the fabricated organic photovoltaic cell "fiber1" are shown linear in figure 4.9, the characteristics were also plotted in semi-log scale, which is depicted in figure 4.10. The black line always presents the measurement recorded under dark conditions, while the red line was recorded under LED irradiation. So what can be seen immediately is, that the two plotted lines (dark, illuminated) are shifted on the x-axis (figure 4.10), which basically means that there is a photocurrent available and the photovoltaic cell is working. It is also possible to read off the figure 4.10 that for the fabricated device "fiber1" the photocurrent gets only slightly bigger under direct illumination than under dark conditions.

To obtain the open-circuit voltage V_{OC} and the short-circuit current density J_{SC} it is easier to look at the semilogarithmic plot (figure 4.10). Under direct lighting it was found that the organic photovoltaic device "fiber1" has an open-circuit voltage of V_{OC} = 80.0 mV and a short-circuit current density of J_{SC} = 0.052 $\frac{mA}{cm^2}$.

To observe the fill factor of the fabricated device, the maximum power point (MPP) was needed. Therefore the power-voltage characteristics were plotted

in figure 4.11 and the highest point in the plot is the MPP. The organic photovoltaic cell "fiber1" showed a maximum power point of V_{MPP} = 36.7 mV and J_{MPP} = 0.031 $\frac{mA}{cm^2}$. The fill factor of the device was now observed with FF = $\frac{V_{MPP} \cdot J_{MPP}}{V_{OC} \cdot J_{SC}}$ = 27.8 %.
The collected results of the fabricated organic photovoltaic cell "fiber1" can be looked up in table 4.7.

Table 4.7: Collected results from the characteristics of "fiber1"

Measure	**Measure description**	**Value**	**Unit**
J_{SC}	short-circuit current density	0.052	$\frac{mA}{cm^2}$
V_{OC}	open-circuit voltage	80.0	mV
J_{MPP}	maximum power point current density	0.031	$\frac{mA}{cm^2}$
V_{MPP}	maximum power point voltage	36.7	mV
FF	Fill Factor	27.8	%

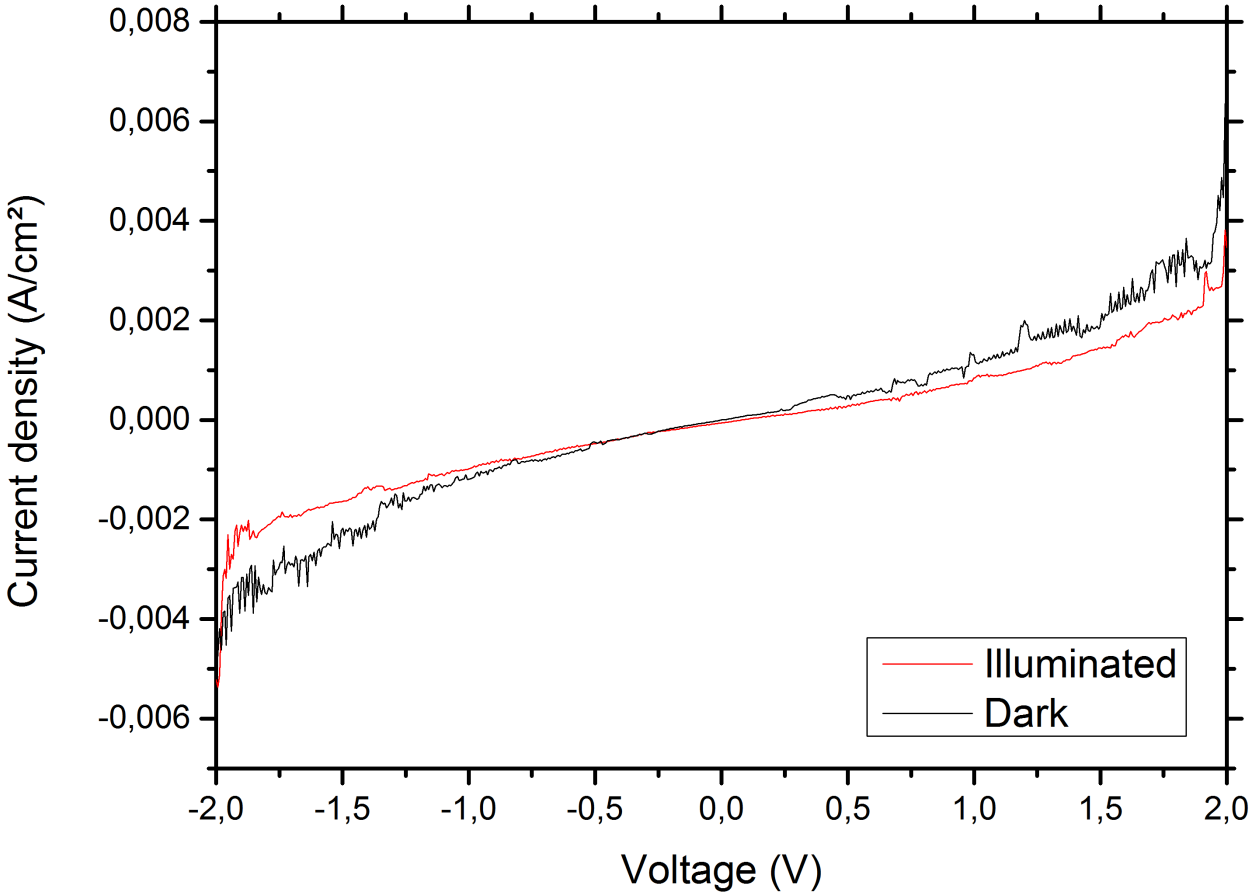

Figure 4.9: Current density-Voltage (J-V) characteristics for fabricated organic photovoltaic cell "fiber1"

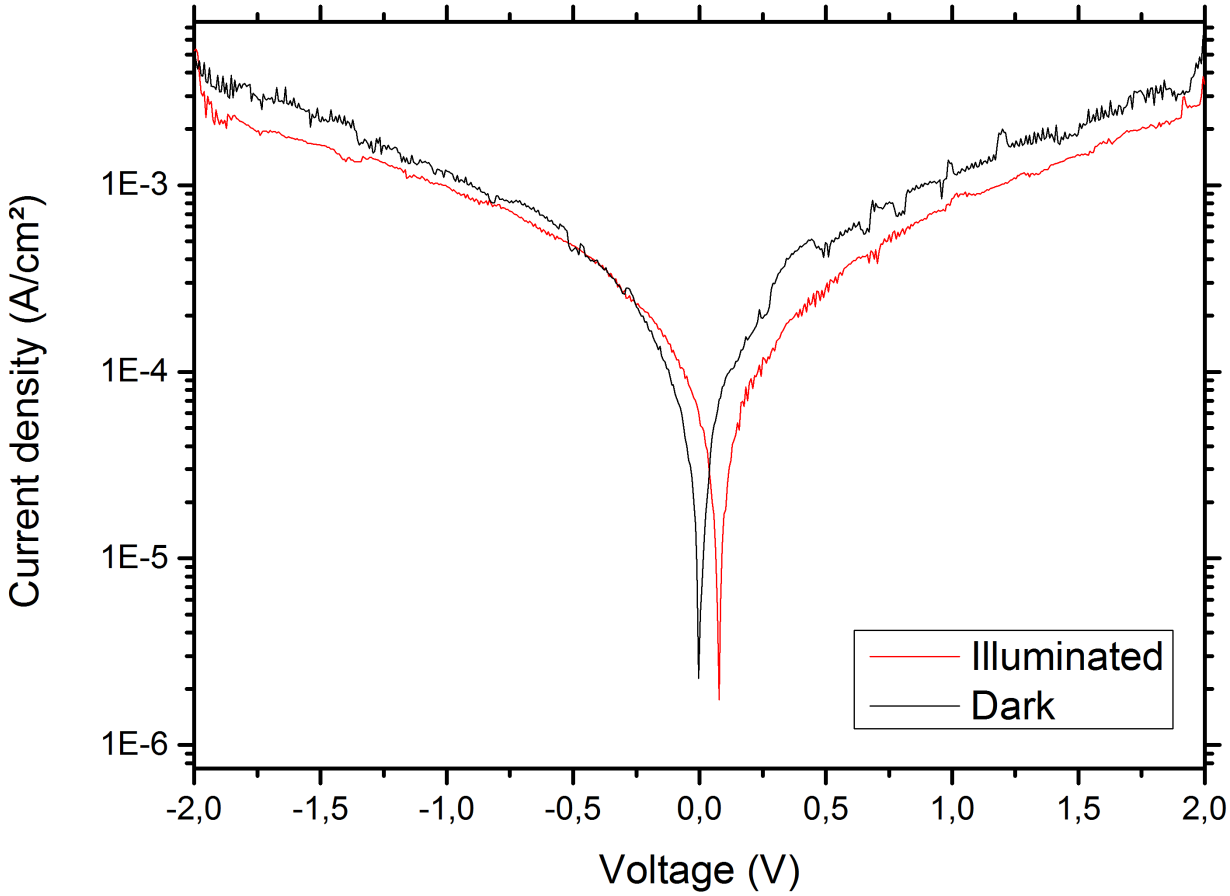

Figure 4.10: Logarithmic J-V-characteristics for fabricated organic photovoltaic cell "fiber1"

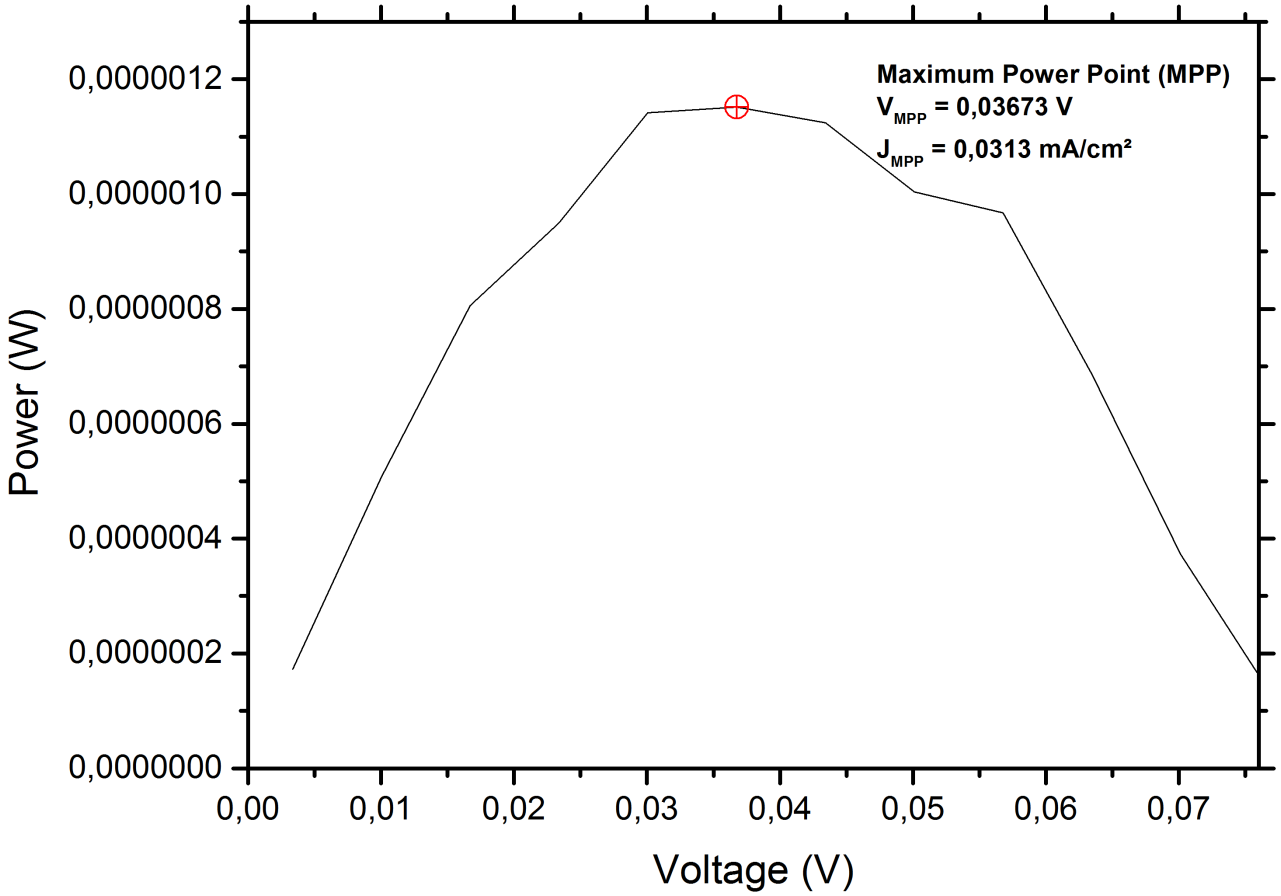

Figure 4.11: Power-Voltage (P-V) characteristics for fabricated organic photovoltaic cell ”fiber1” to get MPP

As well as previously in "fiber1", the current-voltage characteristics for the fabricated organic photovoltaic cell "fiber2" are shown linear scale in figure 4.12 and in semi-log scale in figure 4.13. The black line presents as above the measurement recorded under dark conditions, while the red line was recorded under LED irradiation. So what can be seen again immediately is, that the two plotted lines (dark, illuminated) are also shifted on the x-axis (figure 4.13), which basically means that there is a photocurrent available and the photovoltaic cell is working. It is also possible to read off the figure 4.13 that for the fabricated device "fiber2" the photocurrent gets much bigger under direct illumination than under dark conditions.

To obtain the open-circuit voltage V_{OC} and the short-circuit current density J_{SC} it is easier to look at the semilogarithmic plot (figure 4.13). Under direct lighting it was found that the organic photovoltaic device "fiber2" has an open-circuit voltage of V_{OC} = 83.5 mV and a short-circuit current density of J_{SC} = 0.135 $\frac{mA}{cm^2}$.

To observe the fill factor of the fabricated device, the maximum power point (MPP) was needed. Therefore the power-voltage characteristics were plotted in figure 4.11 and the highest point in the plot is the MPP. The organic photovoltaic cell "fiber2" showed a maximum power point of V_{MPP} = 45.0 mV and J_{MPP} = 0.062 $\frac{mA}{cm^2}$. The fill factor of the device was now observed with FF = $\frac{V_{MPP} \cdot J_{MPP}}{V_{OC} \cdot J_{SC}}$ = 25.0 %.

The collected results of the fabricated organic photovoltaic cell "fiber2" can be looked up in table 4.8.

Table 4.8: Collected results from the characteristics of "fiber2"

Measure	**Measure description**	**Value**	**Unit**
J_{SC}	short-circuit current density	0.135	$\frac{mA}{cm^2}$
V_{OC}	open-circuit voltage	83.5	mV
J_{MPP}	maximum power point current density	0.062	$\frac{mA}{cm^2}$
V_{MPP}	maximum power point voltage	45.0	mV
FF	Fill Factor	25.0	%

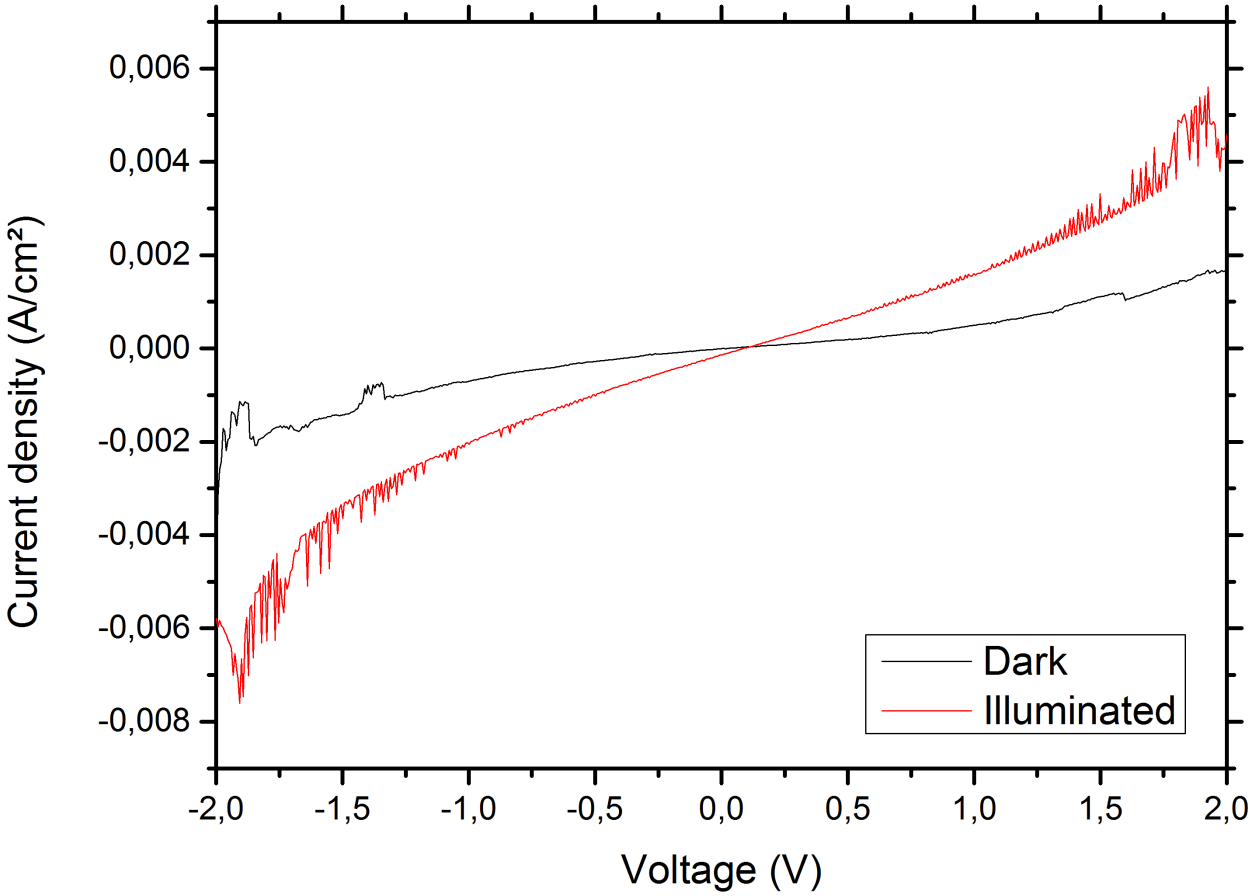

Figure 4.12: Current density-Voltage (J-V) characteristics for fabricated organic photovoltaic cell "fiber2"

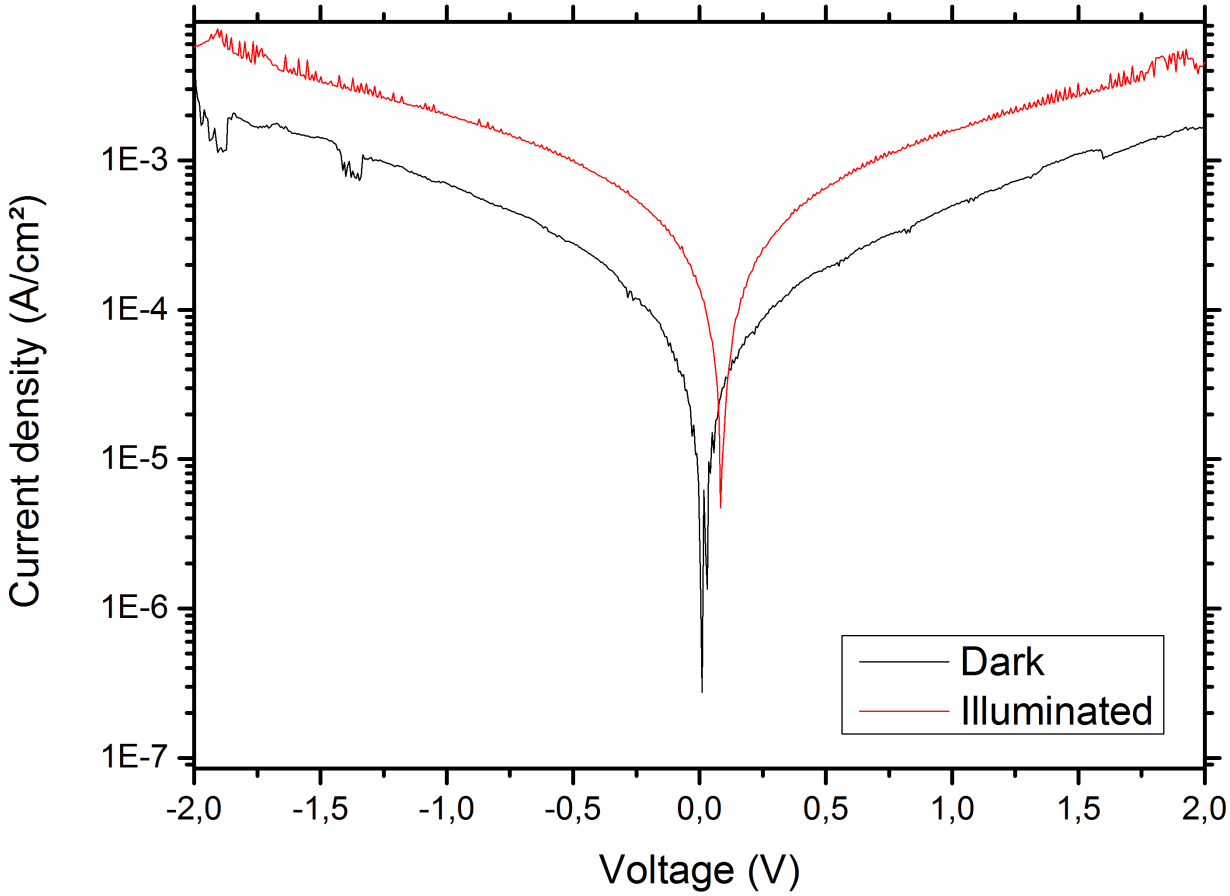

Figure 4.13: Logarithmic J-V-characteristics for fabricated organic photovoltaic cell "fiber2"

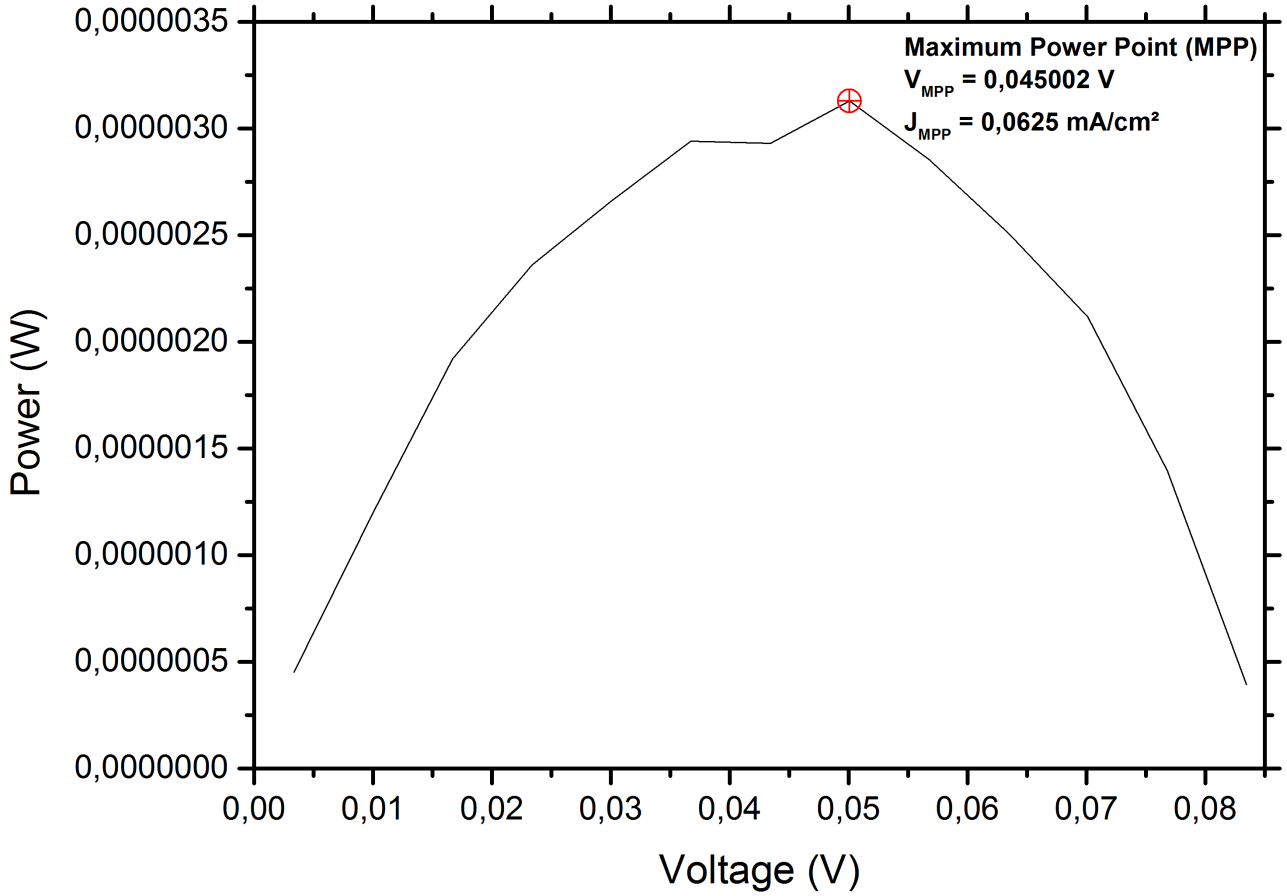

Figure 4.14: Power-Voltage (P-V) characteristics for fabricated organic photovoltaic cell ”fiber2” to get MPP

4.3 Large scale manufacturing process

The methods used for the fabrication of the organic photovoltaics based on cellulose fibers focus on scalability in terms of being usable in a roll-to-roll process as it can be seen in figure 4.15 [8].
First a mono-filament yarn represents the substrate for the fabrication process

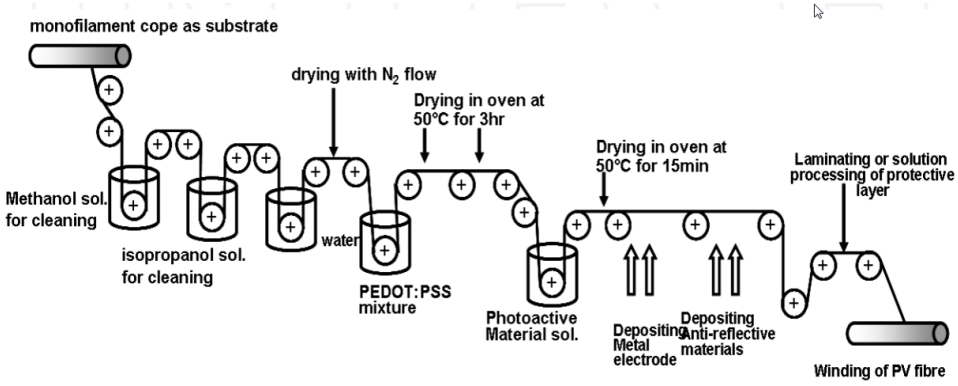

Figure 4.15: Standardized roll-to-roll manufacturing process for a organic photovoltaic fiber [8]

of organic solar cells based on fibers, but instead of using a mono-filament yarn the manufacturing process could also start directly after the fabrication of the viscose fiber, so that the roll-to-roll manufacturing process will never be interrupted. Afterwards the fiber is purged in two baths, first in a bath containing methanol solution and then in a bath containing isopropanol solution. Then the purged mono-filament is cleaned with distilled water and afterwards dried under dry nitrogen atmosphere. Next the fiber is dipped in another bath containing the hole conduction material PEDOT:PSS, thereon another drying process takes place (50°C for 3 hr). Another bath follows as the next step, it contains the photoactive material, followed by another drying process in oven(50°C for 15 min). In the end the metal electrode is thermally evaporated on the fiber and finally an antireflective layer and a protective layer

are applied on the fiber surface. As a result of this standardized manufacturing process an organic solar cell based on fibers is fabricated and can be used for power harvesting [8].

This manufacturing process is called roll-to-roll printing, it has the advantage of very low cost but it also has some disadvantages like the much lower resolution than techniques such as photo-lithography. The challenges for this process are to find materials that can be easily roll printed and that have the necessary electronic and other characteristics.

By looking at this whole standardized process [8], we can check which subprocesses are in principle at the moment possible to have a non-stop continuous manufacturing process in our laboratory. First the cleaning process is no problem, then also bringing on the PEDOT:PSS layer is no problem. Also the active layer should not be a problem, but then one gets to the point where it is not possible to have a non-stop continuous manufacturing process. It is the deposition of the aluminum electrode, because for evaporating aluminum a vacuum is needed and therefore the manufacturing process has to be interrupted. For our low-scale manufacturing this is not a problem, but for large scale manufacturing one has to think about other depositing methods, where no vacuum is needed (see chapter 6).

5 Application fields for an organic photovoltaic cell

Before going on with the discussion, some application fields for an organic photovoltaic device based on cellulose fibers will be shown to answer the question why someone would need them. So if one has a working device, what are the applications for such organic photovoltaic cells.

5.1 Textile industry

An important application field for organic photovoltaic fibers is the textile industry. The technology used therefore is called solar clothing where the solar energy is converted to electrical energy through integrated organic photovoltaic fibers [35]. Integration of such photovoltaic fibers into clothing can supply a new energy source for wearable electronic gadgets. That means that such a solar clothing is the most progressed path of supplying electricity far away from any power supply. What also helps now is that the energy demand for wearable electronic gadgets is at the moment low enough that solar clothing can power most of these devices [36].
Organic photovoltaic fibers are the most qualified ones to textile structures

within all the photovoltaic technologies. They have a lot of nice properties which are favorable for textile structures, like the high flexibility, the low weight, low cost and usage performance. Basically there are two main methods how to implement organic photovoltaic into textile structures [37]:

1. In the first approach the organic photovoltaic cell is fabricated somewhere else and afterwards integrated into the textiles structures by using different methods (patching for example). Contacts between the organic photovoltaic cells are performed using copper wires, which can be also sewn into the textile structures. In the figure 5.1 one can see organic photovoltaic cells integrated into a dress and belt by using the patching method [37].

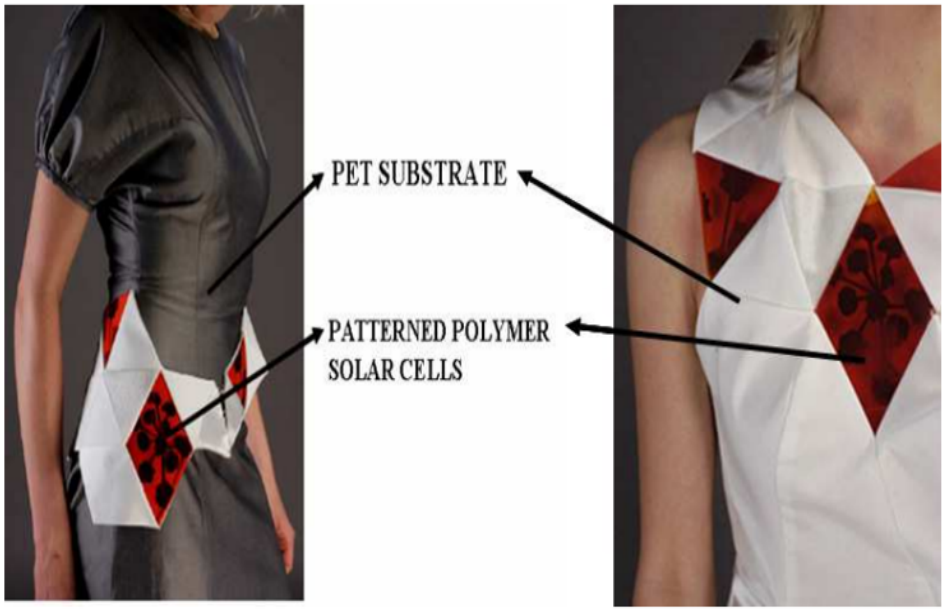

Figure 5.1: Patterned polymer cell within the textile industry [37]

2. Within the second method the organic photovoltaic cell is created directly on the fiber, like it is done in this master thesis. So the fibers themselves can be used directly as yarn and then fabricate the textile structures [37].

5.2 Agriculture industry

Another application field is the agricultural sector, the organic photovoltaic fibers can provide enough electrical energy to power sensors and actuators. That means that for example one is able to control important parameters for growth like stream of air, air moisture, watering and so on without having a main supply. Another possible advantage is to expand the growing cycle by using low level heat produced by energy from organic photovoltaic cells. As a result by using organic photovoltaics one will obtain improved crop yield, more income, better quality and maybe also new products [38].

Figure 5.2: Possible application field: agricultural sector

5.3 Disaster or humanitarian relief

Especially in times like this, it is important that one can support people who lose their homes unpredictable. While there are a lot of options how they have lost their homes (war, earthquake, flooding...), most of these occurrences happen in third world countries. After loosing their home they are normally sheltered in tents and that is exactly the point at which one an help them. As described in section 5.1 one can provide tents where the organic photovoltaic cells are directly integrated into them and therefore they are able to save energy throughout the day an use the energy during night. Such a possible tent can be seen in image 5.3. If there are already tents available, it is also possible to cover them with organic photovoltaic shields.

Figure 5.3: Phototvoltaic fibers integrated in a tent for disaster/humanitarian relief [37]

5.4 Construction sector

Also an important application field is the construction sector, here the organic photovoltaics can be integrated into buildings (in facades, on roofs), called "Building Integrated Organic Photovoltaics" (BIOPV). The biggest advantages within this application field is first the lightness of the organic solar cells and secondly the flexibility of such devices, so it is suitable for all roof structures and facade forms [15]. Another benefit is that an organic solar cell will not crack. In figure 5.4 a BIOPV installation at the Heliatek headquarter in Dresden is shown.

Figure 5.4: Building integrated organic photovoltaic (BIOPV) [39]

6 Discussion

In this chapter first some discussion points regarding the fabrication and results of organic photovoltaic cells based on cellulose sheets and fibers will be revealed and how it is possible to improve the quality of such devices. Afterwards also some general possibilities for improving lifetime, efficiency and stability of organic solar photovoltaics will be discussed. So this chapter will be structured into three parts → Organic photovoltaic cells based on cellulose sheets, organic photovoltaic cells based on cellulose fibers and a general part.

Organic photovoltaic cells based on cellulose sheets

By comparing the results for the organic photovoltaic cells based on cellulose sheets V_{OC} = 0.40 V and FF = 36 % with the results from Kopeiniks thesis [16] V_{OC} = 0.18 V and FF = 30 % it was proven that the fabrication method Kopeinik was using is working. What can be said is that the results reported in this master thesis are a bit better across-the-board, which is perhaps like that because Kopeinik has further diluted the silver nanowires with isopropanol and therefore also the resistance from Kopeiniks devices was slightly bigger. But if one now compares the received results with literature from [31] with V_{OC}

= 0.52 V and FF = 52 % and [40] with the results V_{OC} = 0.60 V and FF between (33 - 54) % one can see that the values are partially significantly higher, so there is still improvement potential available. One big possibility for improvement is the fact that within this master thesis we were using low light illumination due to using a LED of the company OSRAM.
Another option for improvement is described in literatures [41] and [42]. In them it is described that plain mechanical pressing could lead to an increase in the conductance of the silver nanowires film and therefore to a reduction of the resistance. So in turn a lower resistance would increase the quality of the solar cells.
In [42] it is also shown that due to the mechanical pressing also surface roughness decreases, which has the further advantage that the amount of short circuits should also decrease.
However, it has been shown that conductive cellulose sheets can be used as semitransparent electrode for organic photovoltaic cells. So in a short summary, it can be said that the produced organic photovoltaic cells based on cellulose sheets showed quite proper performance and of course there is still room for improvement.

Organic photovoltaic cells based on cellulose fibers

As the aluminum electrode is not transparent the overall geometry shown in figure 4.7 had to be used. However, this geometry is harmful to the performance of the photovoltaic cell, because the electron hole pairs created in the P3HT:PCBM layer have to travel a very long way to the respective electrodes. This greatly enhances the recombination of the electron hole pairs leading to very low performance of the photovoltaic devices. The fairly poor values of

the organic photovoltaic cells based on cellulose fibers J_{SC} = 0.135 mA, V_{OC} = 83.5 mV, FF = 25 % respectively J_{SC} = 0.052 $\frac{mA}{cm^2}$, V_{OC} = 80.0 mV and FF = 28 % are probably to a large part due to this unfavorable geometry of the device depicted in figure 4.7.

So it has to be found another possibility where a transparent electrode is used for fabrication. In literature [43], [44], [45] and [46] an alternative concept is presented where a low temperature solution process allows to use transparent conductive oxides (TCO) as an electrode. If the outer electrode is built with such a TCO instead of aluminum the performance of the devices will increase probably significantly, most likely the performance will be in the order of the fabricated devices based on cellulose sheets.

As the depositing of aluminum is the only process step that is not scalable to a roll-to-roll process as described in 4.3, a low temperature solution based TCO could solve this problem as there is no vacuum chamber needed. Another possible attempt for a flexible transparent outer electrode that could be processed roll-to-roll could be graphene like it is described in [47] and [48].

General discussion and outline

When talking about the performance of organic photovoltaic cells, two essential factors are important. The first keyword is the efficiency, while silicon solar cells have reached efficiencies in the order of 25 % [49], organic solar cells are still behind with efficiencies between (10 - 15) % [50].

So in order to increase the efficiency of the fabricated devices within this master thesis there are various options which should be explored in future:

1. **Anti reflective coating:**

   With an anti reflective coating is has been shown in literature [51], [52]

and [53] that is it possible to enhance the efficiency significantly. This enhancement is applicable for a broad range of incidence angles and saves the apathy of organic photovoltaics against skewed incident light [51].

2. **Use MDMO-PPV:PCBM instead of P3HT:PCBM:**
   In literature [37], [54] and [55] it has been reported, that using MDMO-PPV:PCBM as an active layer for organic photovoltaic cells would also lead to an improvement of efficiency.

The second keyword is the lifetime, whilst inorganic solar cells last on the order of 25 years, organic photovoltaic cells still have problems to last a year, because of the interaction between the molecules and water and oxygen [56]. Therefore, different approaches must be taken into consideration to protect the organic solar cells from degradation:

1. **Encapsulating**
   As mentioned before a big detriment of organic photovoltaic cells is the susceptibility of photoactive layer and top electrode to hydrogen and oxygen. Therefore, in literature [57], [58] and [59] a method for flexible encapsulating the organic photovoltaic cell is shown. This encapsulating will raise the shelf lifetime significantly, for example in [59] from a few hours to more than 3000 hours.
2. **Anti reflective coating:**
   An anti reflective coating would also improve the overall lifetime, because the coating would also serve as a UV-barrier and therefore reduce the rate of degradations as it is described in [53].

7 Summary

Within this master thesis the fabrication of organic photovoltaic cells based on cellulose sheets and fibers was described. After fabrication the performance of the organic photovoltaic cells was investigated. In order to make the cellulose substrates conductive they were coated with silver nanowires. While the conductive cellulose sheets showed a mean electrical resistance $< 100\ \Omega$, the conductive cellulose fibers had a mean electrical resistance $< 50\ \Omega$.
By comparing the results for organic photovoltaic cells based on cellulose sheets with the results from Kopeinik [16] it was shown that the fabrication method is working and that the received results within this thesis are slightly better. The received results for the fabricated devices can be seen in table 7.1. So it has been shown that conductive cellulose sheets can be used as semitransparent electrode for organic photovoltaic cells and the fabricated devices showed quite proper performance but of course there is still room for improvement.

Against the performance of the cellulose sheets devices the cellulose fiber devices showed fairly poor values. The problem was that the aluminum electrode is not transparent and therefore the overall geometry shown in figure 4.7 had to be used. However, this geometry is harmful to the performance of the photovoltaic cell and explains to a large degree these fairly poor values. The received results for the organic photovoltaic cells based on cellulose fibers can

Table 7.1: Collected results of the fabricated organic photovoltaic cells based on cellulose sheets

Measure	**Measure description**	**"paper1"**	**"paper2"**
J_{SC}	short-circuit current density	1.03 $\frac{mA}{cm^2}$	0.517 $\frac{mA}{cm^2}$
V_{OC}	open-circuit voltage	0.40 V	0.29 V
J_{MPP}	maximum power point current density	0.647 $\frac{mA}{cm^2}$	0.151 $\frac{mA}{cm^2}$
V_{MPP}	maximum power point voltage	0.23 V	0.21 V
FF	Fill Factor	36.2 %	36.5 %

be seen in table 7.2. As mentioned already in the discussion, there is still room

Table 7.2: Collected results of the fabricated organic photovoltaic cells based on cellulose fibers

Measure	**Measure description**	**"fiber1"**	**"fiber2"**
I_{SC}	short-circuit current	0.052$\frac{mA}{cm^2}$mA	0.135 $\frac{mA}{cm^2}$
V_{OC}	open-circuit voltage	80.0 mV	83.5 mV
I_{MPP}	maximum power point current	0.031 $\frac{mA}{cm^2}$	0.062 $\frac{mA}{cm^2}$
V_{MPP}	maximum power point voltage	36.7 mV	45.0 mV
FF	Fill Factor	27.8 %	25.0 %

for improvement and for the future one has to focus on three keyfacts: process, efficiency, and stability.

Appendix

Material specification sheets

Bramante – hollow viscose fibre

Bramante is a segmented hollow viscose fibre which is collapsed in the dry state and swells when wetted.

Bramante has an outstanding water absorption and retention capacity. Even under pressure, re-wetting is minimized as the water is firmly incorporated in the fibres' cavities.
Bramante is ideal for all applications which require high absorbency, e.g. for hygiene and medical applications as well as for absorbent textiles.
Its dye pickup is approximately 3 times higher than for standard viscose.

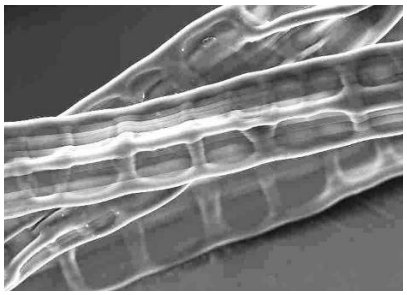

SEM image of Bramante

Applications:

Bramante can be used in 100% or in blends with other fibres, such as viscose, cotton or synthetics for:

- Functional, moisture absorbing and regulating textiles and nonwovens
- Wound dressings
- Tampons
- Incontinence products
- Absorbent pads
- Wipes for household and personal care (wet / dry)

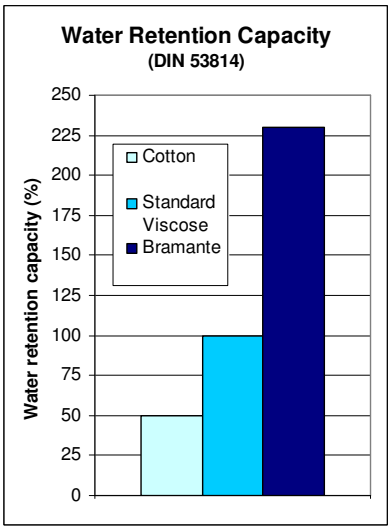

Processing

Bramante can be processed on all common textile, nonwoven and wetlaid technologies

Properties / Availability:

Tenacity (cN / tex)	16 – 18
Elongation at break (%)	20 – 25
Water retention (%)	220 – 360

Decitex	2.1, 3.3
Staple (mm)	40, 60 tow
Lustre	low

Other dtex / staple lengths are available on request.

For more information about our products please email to: functionalfibres@kelheim-fibres.com or call Germany +49-9441-99353. Please visit also our website www.kelheim-fibres.com . 09/2011

SIGMA-ALDRICH®
sigma-aldrich.com

3050 Spruce Street, Saint Louis, MO 63103, USA
Website: www.sigmaaldrich.com
Email USA: techserv@sial.com
Outside USA: eurtechserv@sial.com

Product Specification

Product Name:
Poly(3,4-ethylenedioxythiophene)-poly(styrenesulfonate) - 1.1% in H_2O, neutral pH, high-conductivity grade

Product Number: **739324**

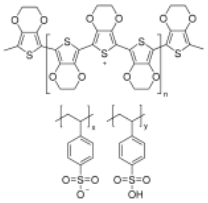

TEST	Specification
Appearance (Color)	Dark Blue to Very Dark Blue
Appearance (Form)	Liquid
Proton NMR spectrum	Conforms to Structure
pH	6.0 - 8.0
Viscosity	≤ 70 cps
Temperature	
Temperature (viscosity), Deg C	
Solid Content	1.0 - 1.2 %
Miscellaneous Assay	≤ 100
Resistivity, Ohm/sq	
Note	Note
Product of Agfa-Gevaert N.V.	

Specification: PRD.1.ZQ5.10000034896

SIGMA-ALDRICH®
sigma-aldrich.com

3050 Spruce Street, Saint Louis, MO 63103, USA
Website: www.sigmaaldrich.com
Email USA: techserv@sial.com
Outside USA: eurtechserv@sial.com

Product Specification

Product Name:
Silver nanowires - diam. × L 115 nm × 20–50 µm, 0.5% (isopropyl alcohol suspension)

Product Number: **739448**
CAS Number: 7440-22-4

Formula: Ag
Formula Weight: 107.87 g/mol

TEST	Specification
Appearance (Color)	Grey
Appearance (Form)	Suspension
Proton NMR spectrum	Conforms to Structure
ICP Major Analysis Confirms Silver Component	Confirmed
Length 20-50um	Confirmed
Diameter 115 nm + /-15 nm	Confirmed
Concentration 0.5 wt.% in IPA	Confirmed

Specification: PRD.0.ZQ5.10000044099

Specification sheet for Poly(3-hexylthiophene-2,5-diyl), regioregular

CAS 104934-50-1

	Molecular Weight (Mw)	Regioregularity (RR)	Polydispersity (PDI)
4002-E	50-70K	91-94%	2.0-2.5
4002-EE	50-70K	91-94%	2.0-2.5
RMI-001E	Batches from 30K to 100K	96%	2.0-2.3
RMI-001EE	Batches from 30K to 100K	96%	2.0-2.3
RMI-002E	27K-37K	89%	1.5-1.7
RMI-002EE	27K-37K	89%	1.5-1.7

EE grades have undergone additional purification

PCBM

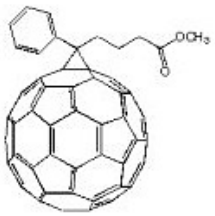

Order Code: M111

MSDS sheet

Quantity 1 g

Purity >99% Purity

Price

excluding Taxes

Add to Cart

£149.00

Share Share Tweet Pin it Fancy +1

Product Description - PCBM

[6,6]-Phenyl-C61-butyric acid methyl ester (or PCBM).

A high quality **PCBM** ideal for OPVs. The 99% purity PCBM has produced efficiencies of over 4.5% in our own laboratories and is recommended for general OPV use. The 99.5% purity PCBM is recommended for OFET applications where the highest crystallisation and mobility is required.

Specifications	
Mw	911 g/mol
Purity	>99% or >99.5%
CAS number	160848-22-6

List of Figures

List of Tables

Bibliography

[1] EIA. "International Energy Outlook 2011." In: *Table A2* (2011) (cit. on p. 1).

[2] Tingzhen Ming et al. "Fighting global warming by climate engineering: Is the Earth radiation management and the solar radiation management any option for fighting climate change?" In: *Renewable and Sustainable Energy Reviews* 31 (2014), pp. 792–834. DOI: 10.1016/j.rser.2013.12.032 (cit. on p. 2).

[3] *Benefits of Renewable Energy Use*. Union of Concerned Scientist. URL: http://www.ucsusa.org/clean_energy/our-energy-choices/renewable-energy/public-benefits-of-renewable.html#.VzDeJ_mLSUk (visited on 04/28/2016) (cit. on p. 2).

[4] Rabia Ferroukhi et al. "RENEWABLE ENERGY BENEFITS: MEASURING THE ECONOMICS." In: *IRENA* (2016) (cit. on p. 2).

[5] *Why is renewable energy important?* Renewable Energy World. URL: http://www.renewableenergyworld.com/index/tech/why-renewable-energy.html (visited on 03/28/2016) (cit. on p. 2).

[6] Wallace C. H. Choy. *Organic Solar Cells - Materials and Device Physics*. Springer, 2013. ISBN: 978-1-4471-4823-4 (cit. on pp. 3, 4).

[7] Bengston. *SCIENTISTS 3D PRINT NEW SOLAR PANELS WHICH WORK BEST WHEN CLOUDY*. 3DPrint. 2014. URL: https://3dprint.com/1666/scientists-3d-print-new-solar-panels-which-work-best-when-cloudy/ (visited on 05/03/2016) (cit. on p. 3).

[8] A Bedeloglua et al. In: *Synthetic Metals* 159 (2009), pp. 2043–2048 (cit. on pp. 3, 78, 79).

[9] *Core–shell semiconductor nanocrystal*. Wikipedia. 2016. URL: https://en.wikipedia.org/wiki/Core%C3%A2%C2%80%C2%93shell_semiconductor_nanocrystal (visited on 03/05/2016) (cit. on p. 5).

[10] Markus Schwoerer and Hans Christoph Wolf. *Organische Molekulare Festkörper: Einführung in die Physik von pi-Systemen*. 2012. DOI: 10.1002/ange.200585310 (cit. on p. 5).

[11] Guenter Graichen. "Alternative Energien: Solarzellen richtig einsetzen Teil 1 und 2." In: *rfe, Technik & Markt der CE-Branche* 12 (1998) (cit. on p. 6).

[12] *Organic solar cell*. Wikipedia. URL: https://en.wikipedia.org/wiki/Organic_solar_cell (visited on 04/05/2016) (cit. on p. 6).

[13] *General structure of an organic solar cell*. URL: http://www.cstf.kyushu-u.ac.jp/~adachilab/lab/?page_id=3927 (visited on 02/16/2016) (cit. on p. 7).

[14] Askari Mohammad Bagher. "Comparison of organic solar cells and inorganic solar cells." In: *International Journal of Renewable and Sustainable Energy* 3 (2014), pp. 53–58 (cit. on p. 7).

[15] Mario Pagliaro, Giovanni Palmisano, and Rosaria Ciriminna. *Flexible Solar Cells*. John Wiley & Sons, 2008. DOI: 10.1002/cssc.200800127 (cit. on pp. 8, 84).

[16] Heribert Kopeinik. "Organic Diodes and Photovoltaic Cells based on Conductive Cellulose Fiber Networks." MA thesis. Graz University of Technology, 2014 (cit. on pp. 9, 26–28, 30, 33–36, 39, 41, 42, 44, 85, 89).

[17] *Utilizing Carbon Nanotubes to Improve Efficiency of Organic Solar Cells*. University of Maryland. 2006. URL: https://www.google.at/url?sa=t&rct=j&q=&esrc=s&source=web&cd=1&cad=rja&uact=8&ved=0ahUKEwjg-LKMhbnMAhUBGxQKHe2vBTAQFggbMAA&url=http://www.mse.umd.edu/sites/default/files/documents/undergrad/enma490/ENMA490-Final-Presentation-sp06.ppt&usg=AFQjCNGAGsxxW_tbxCvDraD3QErLLTEnvA&sig2=JOkL-NGL3PYjsclYA9bK_A&bvm=bv.121070826,d.d24 (visited on 04/18/2016) (cit. on p. 9).

[18] P. Peumans, A. Yakimov, and S.R. Forrest. "Small molecular weight organic thin-film photodetectors and solar cells." In: *Journal of Applied Physics* 93 (2003) (cit. on p. 9).

[19] *How do polymer solar cells work*. URL: http://plasticphotovoltaics.org/lc/lc-polymersolarcells/lc-how.html (visited on 03/25/2016) (cit. on pp. 10, 11).

[20] David Quéré. "FLUID COATING ON A FIBER." In: *Annual Review of Fluid Mechanics* 31 (1999). DOI: 10.1146/annurev.fluid.31.1.347 (cit. on p. 12).

[21] Binda Magdalena. "Deposition and patterning techniques for Organic Semiconductors." MA thesis. Politecnico di Milano, 2011 (cit. on p. 13).

[22] *Processing techniques for depositing*. 2012. URL: https://stuff.mit.edu/afs/athena.mit.edu/course/3/3.082/www/team2_f02/Pages/processing.html (visited on 04/18/2016) (cit. on p. 14).

[23] Hermenau Martin. "Lebensdaueruntersuchungen an organischen Solarzellen." PhD thesis. Technischen Universität Dresden, 2012 (cit. on p. 16).

[24] Lacramioara Mihaela Popescu. "Fullerene based Organic Solar Cells." MA thesis. University of Groningen, 2008 (cit. on p. 16).

[25] Calvin Woodings. *Regenerated Cellulose Fibres*. CRC Press, 2001 (cit. on pp. 19, 20).

[26] *Eucalyptus fiber by any other name*. 2012. URL: https://oecotextiles.wordpress.com/tag/regenerated-cellulose/ (visited on 04/13/2016) (cit. on p. 21).

[27] Paul W.M. Blom et al. "Small Bandgap Polymers for Organic Solar Cells (Polymer Material Development in the Last 5 Years)." In: *Polymer Reviews* 48 (2008), pp. 531–582. DOI: 10.1080/15583720802231833 (cit. on pp. 20, 23).

[28] *PCBM*. Wikipedia. URL: https://de.wikipedia.org/wiki/PCBM (visited on 02/20/2016) (cit. on p. 22).

[29] *P3HT*. Ossila Ltd, Kroto Innovation Centre, Broad Lane, Sheffield S3 7HQ. URL: http://www.ossila.com/products/p3ht (visited on 04/24/2016) (cit. on p. 22).

[30] *PEDOT:PSS*. Wikipedia. URL: https://en.wikipedia.org/wiki/PEDOT:PSS (visited on 04/19/2016) (cit. on p. 23).

[31] Johannes Krantz et al. "Solution-Processed Metallic Nanowire Electrodes as Indium Tin Oxide Replacement for Thin-Film Solar Cells." In: *Advanced Functional Materials* 21.24 (2011), pp. 4784–4787. DOI: 10.1002/adfm.201100457 (cit. on pp. 41, 85).

[32] Andreas Graff et al. “Silver nanowires.” In: *THE EUROPEAN PHYSICAL JOURNAL D* 34.1 (July 2005), pp. 263–269. DOI: 10.1140/epjd/e2005-00108-7 (cit. on p. 41).

[33] *Bramante – hollow viscose fibre*. Kelheim Fibres. URL: http://www.kelheim-fibres.com/pdf/TDS%20Bramante.pdf (visited on 02/18/2016) (cit. on p. 58).

[34] Fischer WJ et al. “Imaging of the formerly bonded area of individual fibre to fibre joints with SEM and AFM.” In: *Cellulose* 21 (Feb. 2014), pp. 251–260. DOI: 10.1007/s10570-013-0107-0 (cit. on p. 59).

[35] Yong-Hee Lee et al. “Wearable Textile Battery Rechargeable by Solar Energy.” In: *Nano Lett.* 13 (2013), pp. 5753–5761. DOI: 10.1021/nl403860k (cit. on p. 80).

[36] Markus B. Schubert and Juergen H. Werner. “Flexible solar cells for clothing.” In: *Materials Today* 9 (2006), pp. 42–50. DOI: 10.1016/S1369-7021(06)71542-5 (cit. on p. 80).

[37] Leonid A. Kosyachenko. *Solar Cells - New Aspects and Solutions*. InTech, 2011. DOI: 10.5772/1759 (cit. on pp. 81, 83, 88).

[38] Rameshprabu Ramaraj and Natthawud Dussadee. “Renewable Energy Application for Organic Agriculture: A review.” In: *International Journal of Sustainable and Green Energy* 4 (2015), pp. 33–38. DOI: 10.11648/j.ijrse.s.2015040101.15 (cit. on p. 82).

[39] *BIOPV Installation*. Heliatek. 2014. URL: http://www.heliatek.com/de/presse/pressemitteilungen/details/heliatek-verkuendet-groesste-biopv-installation (visited on 05/01/2016) (cit. on p. 84).

[40] Hui Lu et al. “Inkjet printed silver nanowire network as top electrode for semi-transparent organic photovoltaic devices.” In: *Applied Physics Letters* 106 (2015). DOI: 10.1063/1.4913697 (cit. on p. 86).

[41] Takehiro Tokuno et al. "Fabrication of silver nanowire transparent electrodes at room temperature." In: *Nano Research* 4 (2011), pp. 1215–1222. DOI: 10.1007/s12274-011-0172-3 (cit. on p. 86).

[42] Liangbing Hu et al. "Scalable Coating and Properties of Transparent, Flexible, Silver Nanowire Electrodes." In: *ACSNano* 4.5 (2010), pp. 2955–2963 (cit. on p. 86).

[43] CG Granqvist. "Transparent conductors as solar energy materials: A panoramic review." In: *Solar Energy Materials & Solar Cells* 91 (2007), pp. 1529–1598 (cit. on p. 87).

[44] M Hilgendorff et al. "From ZnO colloids to nanocrystalline highly conductive films." In: *J Electrochem Soc* 145.10 (1998), pp. 3632–3637 (cit. on p. 87).

[45] D Kisailus et al. "Kinetically controlled catalytic formation of zinc oxide thin films at low temperature." In: *J Am Chem Soc* 128 (2006), pp. 10276–10280 (cit. on p. 87).

[46] FSF Morgenstern et al. "Ag-nanowire films coated with ZnO nanoparticles as a transparent electrode for solar cells." In: *Appl Phys Lett* 99 (2011) (cit. on p. 87).

[47] Z Wei et al. "Nanoscale tunable reduction of graphene oxide for graphene electronics." In: *Science* 328 (2010), pp. 1373–1376 (cit. on p. 87).

[48] C Zhu et al. "Reducing sugar: New functional molecules for the green synthesis of graphene nanosheets." In: *ACS Nano* 4.4 (2010), pp. 2429–2437 (cit. on p. 87).

[49] Martin A. Green. "The Path to 25 % Silicon Solar Cell Efficiency: History of Silicon Cell Evolution." In: *PROGRESS IN PHOTOVOLTAICS: RESEARCH AND APPLICATIONS* 17 (2009), pp. 183–189. DOI: 10.1002/pip.892 (cit. on p. 87).

[50] M.C. Scharber and N.S. Sariciftci. "Efficiency of bulk-heterojunction organic solar cells." In: *Progress in Polymer Science* 38 (2013), pp. 1929–1940. DOI: 10.1016/j.progpolymsci.2013.05.001 (cit. on p. 87).

[51] Karen Forberich et al. "Performance improvement of organic solar cells with moth eye anti-reflection coating." In: *Thin Solid Films* 516 (2008), pp. 7167–7170 (cit. on pp. 87, 88).

[52] J. E. Nam et al. "Effect of Anti-Reflective Layer in Dye-Sensitized Solar Cells." In: *Applied Mechanics and Materials* 705 (2015), pp. 320–323 (cit. on p. 87).

[53] Pritesh Hiralal et al. "Nanowire-based multifunctional antireflection coatings for solar cells." In: *Nanoscale* 6 (2014), pp. 14555–14562. DOI: 10.1039/c4nr01914h (cit. on p. 88).

[54] Rene A. J. Janssen et al. "Efficient Methano fullerene MDMO-PPV Bulk Heterojunction Photovoltaic Cells." In: *Angew. Chem. Int. Ed.* 42 (2003), pp. 3371–3375. DOI: 10.1002/anie.200351647 (cit. on p. 88).

[55] Charles A. Wilkie, Georges Geuskens, and Victor Manuel de Matos Lobo. *Handbook of Research on Functional Materials: Principles, Capabilities and Limitations*. Apple Academic Press, Feb. 2014 (cit. on p. 88).

[56] Askari Mohammad Bagher, Mirzaei Mahmoud Abadi Vahid, and Mirhabibi Mohsen. "Types of Solar Cells and Application." In: *American Journal of Optics and Photonics* 3.5 (2015), pp. 94–113. DOI: 10.11648/j.ajop.20150305.17 (cit. on p. 88).

[57] Christoph Lungenschmied et al. "Flexible, long-lived, large-area, organic solar cells." In: *Solar Energy Materials & Solar Cells* 91 (2007), pp. 379–384 (cit. on p. 88).

[58] Jongwoon Park. "Thin film encapsulation for flexible organic solar cells." In: *Photovoltaic Specialists Conference* 35 (2010), pp. 1657–1659. DOI: 10.1109/PVSC.2010.5616570 (cit. on p. 88).

[59] G. Dennler et al. "A new encapsulation solution for flexible organic solar cells." In: *Thin Solid Films* 511-512 (2006), pp. 349–353 (cit. on p. 88).